AD-A125 457 AEROELASTIC STABILITY OF A FORWARD SWEPT WING WITH WING TIP STORES(U) AIR FORCE INST OF TECH WRIGHT-PATTERSON AFB OH W G STEELE DEC 82 AFIT/CI/NR-82-69T 1/1

UNCLASSIFIED F/G 20/4 NL

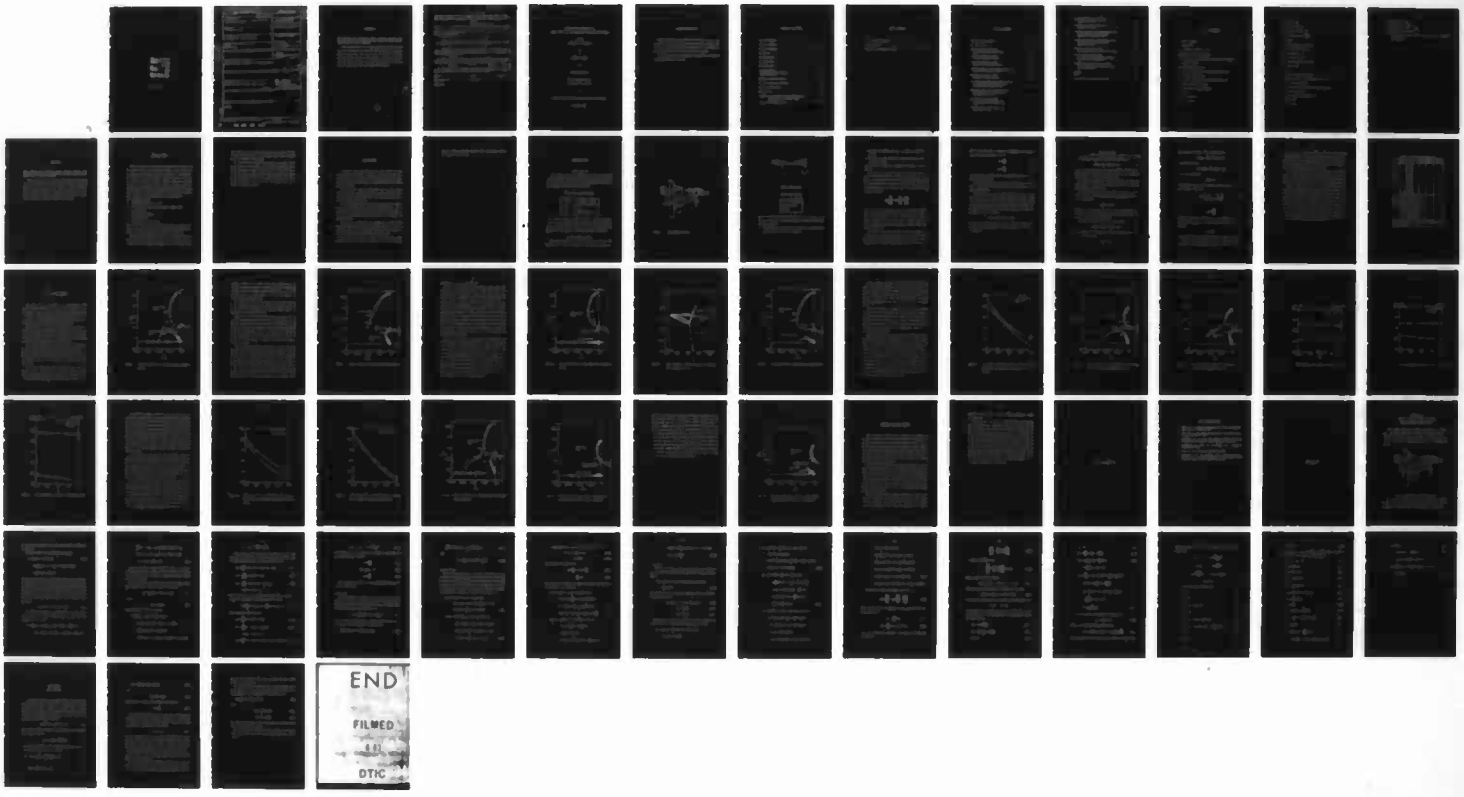

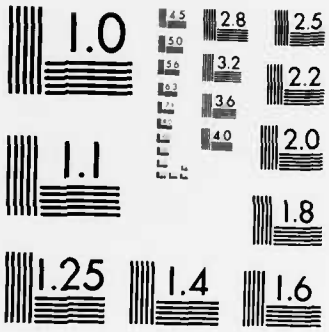

UNCLASS
SECURITY CLASSIFICATION OF THIS PAGE (When Date Entered)

REPORT DOCUMENTATION PAGE

READ INSTRUCTIONS BEFORE COMPLETING FORM

1. REPORT NUMBER: AFIT/CI/NR 82-69T
2. GOVT ACCESSION NO.: AD A125 457
3. RECIPIENT'S CATALOG NUMBER:

4. TITLE (and Subtitle): Aeroelastic Stability of a Forward Swept Wing with Wing Tip Stores
5. TYPE OF REPORT & PERIOD COVERED: THESIS/DISSERTATION
6. PERFORMING ORG. REPORT NUMBER:

7. AUTHOR(s): William Gene Steele
8. CONTRACT OR GRANT NUMBER(s):

9. PERFORMING ORGANIZATION NAME AND ADDRESS: AFIT STUDENT AT: Purdue University
10. PROGRAM ELEMENT, PROJECT, TASK AREA & WORK UNIT NUMBERS:

11. CONTROLLING OFFICE NAME AND ADDRESS: AFIT/NR, WPAFB OH 45433
12. REPORT DATE: Dec 82
13. NUMBER OF PAGES: 56

14. MONITORING AGENCY NAME & ADDRESS (if different from Controlling Office):
15. SECURITY CLASS. (of this report): UNCLASS
15a. DECLASSIFICATION/DOWNGRADING SCHEDULE:

16. DISTRIBUTION STATEMENT (of this Report)
APPROVED FOR PUBLIC RELEASE; DISTRIBUTION UNLIMITED

DTIC ELECTE MAR 10 1983 A

17. DISTRIBUTION STATEMENT (of the abstract entered in Block 20, if different from Report)

18. SUPPLEMENTARY NOTES
APPROVED FOR PUBLIC RELEASE: IAW AFR 190-17
17 Feb 83
LYNN E. WOLAVER
Dean for Research and Professional Development
AFIT, Wright-Patterson AFB OH

19. KEY WORDS (Continue on reverse side if necessary and identify by block number)

20. ABSTRACT (Continue on reverse side if necessary and identify by block number)
ATTACHED

DD FORM 1 JAN 73 1473 EDITION OF 1 NOV 65 IS OBSOLETE UNCLASS
SECURITY CLASSIFICATION OF THIS PAGE (When Date Entered)

AD A125457

DTIC FILE COPY

ABSTRACT

Steele, William Gene, M.S.A.A.E., Purdue University, December 1982. Aeroelastic Stability of a Forward Swept Wing Aircraft with Wing Tip Stores. Major Professor: Terrence A. Weisshaar.

When studying stability of an aircraft, a quasi-steady aerodynamic model is often used. In this study, the results of a stability analysis of an unrestrained flexible forward swept wing aircraft using an unsteady aerodynamic formulation will be compared to results obtained with a similar, but quasi-steady, aerodynamic formulation. In addition, the potential effects of wing tip stores on forward swept wing aircraft stability will be explored.

AFIT/CI/NR 82-69T

AFIT RESEARCH ASSESSMENT

The purpose of this questionnaire is to ascertain the value and/or contribution of research accomplished by students or faculty of the Air Force Institute of Technology (ATC). It would be greatly appreciated if you would complete the following questionnaire and return it to:

AFIT/NR
Wright-Patterson AFB OH 45433

RESEARCH TITLE: Aeroelastic Stability of a Forward Swept Wing with Wing Tip Stores

AUTHOR: William Gene Steele

RESEARCH ASSESSMENT QUESTIONS:

1. Did this research contribute to a current Air Force project?

( ) a. YES ( ) b. NO

2. Do you believe this research topic is significant enough that it would have been researched (or contracted) by your organization or another agency if AFIT had not?

( ) a. YES ( ) b. NO

3. The benefits of AFIT research can often be expressed by the equivalent value that your agency achieved/received by virtue of AFIT performing the research. Can you estimate what this research would have cost if it had been accomplished under contract or if it had been done in-house in terms of manpower and/or dollars?

( ) a. MAN-YEARS _____ ( ) b. $_____

4. Often it is not possible to attach equivalent dollar values to research, although the results of the research may, in fact, be important. Whether or not you were able to establish an equivalent value for this research (3. above), what is your estimate of its significance?

( ) a. HIGHLY SIGNIFICANT ( ) b. SIGNIFICANT ( ) c. SLIGHTLY SIGNIFICANT ( ) d. OF NO SIGNIFICANCE

5. AFIT welcomes any further comments you may have on the above questions, or any additional details concerning the current application, future potential, or other value of this research. Please use the bottom part of this questionnaire for your statement(s).

NAME GRADE POSITION

ORGANIZATION LOCATION

STATEMENT(s):

AEROELASTIC STABILITY OF A FORWARD SWEPT WING AIRCRAFT WITH WING TIP STORES

A Thesis

Submitted to the Faculty

of

Purdue University

by

William Gene Steele

In Partial Fulfillment of the

Requirements for the Degree

of

Master of Science in Aeronautical and Astronautical Engineering

December 1982

ACKNOWLEDGMENTS

I wish to express my deepest gratitude to Dr. Terrence A. Weisshaar who as chairman of my committee provided continuous guidance throughout this study. I would also like to extend my sincere thanks to the other members of my committee, Dr. Henry T. Yang and Dr. Charles M. Krousgrill.

I would like to express my appreciation to Terri Denison for her patience in typing and editing the manuscript.

TABLE OF CONTENTS

LIST OF TABLES

LIST OF FIGURES

LIST OF SYMBOLS

b Wing semi-chord

c Wing chord

c_{l_α} Sectional lift curve slope of wing

C(k) Theodorsen's circulation function

d Distance between canard/tail center of pressure and aircraft c.g.

e Wing static margin

EI Bending stiffness parameter

f Mode shape of fundamental wing flexural vibration mode

h Wing bending displacement

I_α Mass moment of inertia of wing about the reference axis

I_s Mass momen of inertia of store

I_F Mass moment of inertia of fuselage

i $\sqrt{-1}$

k reduced frequency

l Wing semi-span

M_F Fuselage mass

M_T Total aircraft mass

m Wing mass per unit length

q Dynamic pressure, $q = \frac{1}{2}\rho V^2$

q_n $q\cos^2\Lambda$

r_α Radius of gyration of wing section

r_s Radius of gyration of store

S Wing planform area

V Free stream velocity

V_{DC} Clamped wing divergence velocity

V_F Flutter velocity

V_n $V\cos\Lambda$

w Aircraft c.g. plunge displacement

x Distance between line of aerodynamic centers of wing and c.g.

x_s Store position on wing tip

z Distance between wing root line of centers of mass and c.g.

β Store/wing mass ratio

θ Pitch rotation about the aircraft c.g.

ρ Air density

Λ Wing sweep

ω Frequency of oscillation

ω_o Wing cantilever natural frequency

ω_p Uncoupled plunge natural frequency

μ Wing/fuselage mass ratio. Note that the total mass of the aircraft is $M_T = M_F(1+\mu)$

ABSTRACT

Steele, William Gene, M.S.A.A.E., Purdue University, December 1982. Aeroelastic Stability of a Forward Swept Wing Aircraft with Wing Tip Stores. Major Professor: Terrence A. Weisshaar.

When studying stability of an aircraft, a quasi-steady aerodynamic model is often used. In this study, the results of a stability analysis of an unrestrained flexible forward swept wing aircraft using an unsteady aerodynamic formulation will be compared to results obtained with a similar, but quasi-steady, aerodynamic formulation. In addition, the potential effects of wing tip stores on forward swept wing aircraft stability will be explored.

INTRODUCTION

Mission requirements for modern tactical fighter aircraft dictate the need for continued research in advanced fighter technology. Recent studies have shown that aeroelastic divergence of swept forward wings can be controlled by the application of aeroelastic tailoring of composite structures. A study by N.J. Krone (1) showed that tailored composites could avoid aeroelastic divergence of the forward swept wing with little or no weight penalty. The Defense Advanced Research Projects Agency (DARPA) funded several forward swept wing studies. These studies identified several advantages for a forward swept wing aircraft. Krone summarized these advantages as follows:

1) Configuration flexibility
2) Significantly higher maneuver - L/D.
3) Lower trim drag-increased supersonic range for variable sweep.
4) Lower stall speed.
5) Better low speed handling.
6) Virtually spin proof.
7) Volume benefits - lower wave drag.

Also, the use of active controls for flutter suppression and enhanced ride quality has become more feasible. Thus the forward swept wing (FSW) fighter has become a potentially feasible design candidate for a fighter aircraft.

This study has two principal objectives. First it will examine differences between flutter predictions that may arise from the use of quasi-steady motion to model the motion dependent aerodynamic forces on the flexible FSW

aircraft and the use of an unsteady representation of these forces. In addition, the study will identify some of the likely effects of the inclusion of wing tip stores on the stability of a FSW aircraft.

For this study a three degree-of-freedom model is used; this model has body freedoms in pitch and plunge and a single fundamental bending mode. Torsional deformation is deleted to isolate the effect of bending flexibility on the forward swept wing stability problem. A small tip missile is also included in the analytical model. This "store" is rigidly attached to the wing tip. Important parameters to be varied include: wing position relative to the aircraft c.g.; and tip store position.

BACKGROUND

In preliminary stability and control studies the analyst focuses on the rigid body motions of the aircraft. In contrast to this, the flutter analyst is concerned primarily with the elastic vibratory motions of the aircraft structure. For a rigorous aeroelastic study, however, the rigid-body and the elastic modes should be considered.

A study by R.L. Swaim (2) showed that there is a great deal of interaction, known as "Aerodynamic Coupling", between the rigid-body motion and the elastic modes of a flexible vehicle. This interaction can drive one or more of the modes involved unstable.

In a study by Weisshaar and Zeiler (3) on the potential vehicle instability modes of a flexible FSW aircraft, quasi-steady aerodynamics were used to model the unsteady aerodynamic loads. This assumption was made based on the fact that the frequencies of vehicle motion for this type of analysis were generally quite low.

This study will compare the aeroelastic stability results of a FSW aircraft using both unsteady and quasi-steady aerodynamic theories to model the aerodynamic loads. Also, it will investigate the effect of a wing tip store, and the stores chordwise position on the stability of the FSW aircraft.

Future fighter aircraft may be designed with forward swept wings, therefore the need to study the effects of wing tip stores on forward swept wing

aircraft is extremely important. Related to this is the problem of how to model motion dependent airloads.

METHODOLOGY

Model Parameters

The planform geometry of the aircraft aeroelastic stability analysis model is shown in Figure 1. Several of the parameters in Figure 1 will remain fixed for the analyses that will be presented. These fixed parameters along with the mass properties of the aircraft, are given in Table 1.

Table 1 Fixed Aircraft Parameters

b = 2.18 ft.	m = 1.656 slugs/ft. (800 lb)
l = 15 ft	M_T = 496.89 slugs (16,000 lb)
d = 4.5 ft	μ = 0.11
Λ = -30 °	I_α = 138.67 lb–ft^2/ft

Figure 2 shows a typical tip missile or "store" for a light-weight fighter aircraft. The mass properties of this store are given in Table 2. The properties of this aircraft model were considered as suitable for a potential light-weight fighter aircraft. Any similarity to an actual aircraft design is coincidental.

Aeroelastic Equations of Motion

The planform geometry of the aircraft model is shown in Figure 1. The flexible wing has a uniform chord and sweep. The junction between the wing

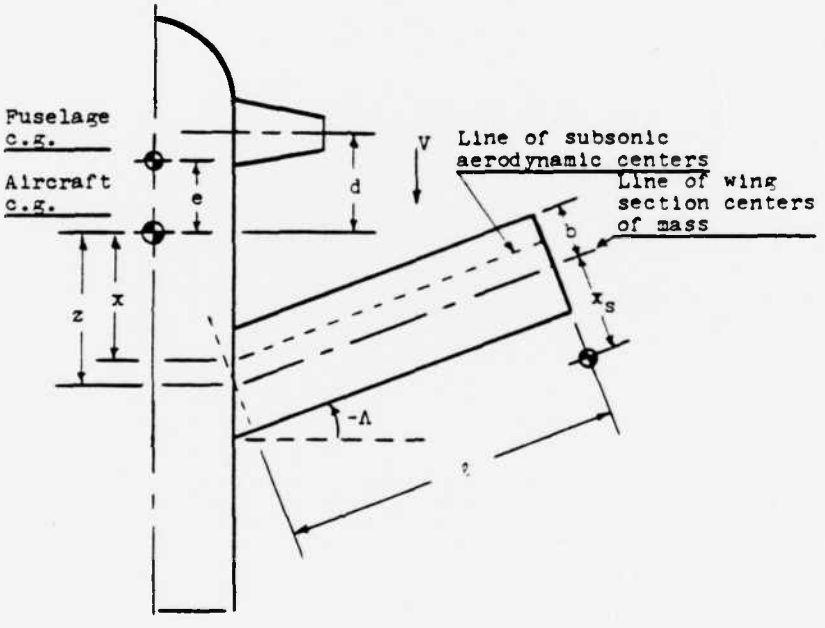

Figure 1 Model Planform Geometry

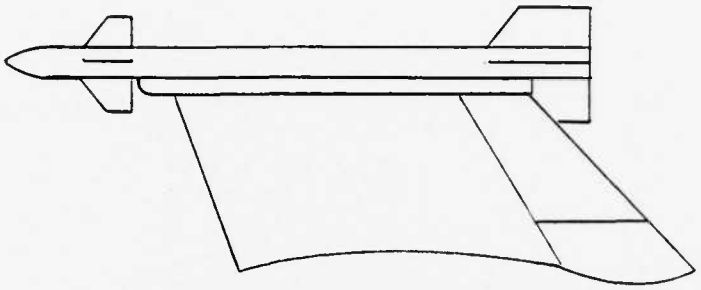

Figure 2 Wing Tip Store

Table 2 Store Properties

M_S = 7.45 slugs (240 lb)
I_S = 170.13 lb–ft^2
β = 0.30

quarter chord line and the side of the fuselage is located at a distance x aft the aircraft c.g. The swept semi-span of the wing is l. The model has three degrees of freedom. These are:

1) Upward displacement of the aircraft c.g., denoted as w, measured positive upward. This is the *plunge* degree of freedom.

2) Pitching of the fuselage about the c.g., denoted θ, measured positive nose-up.

3) Bending of the wings, denoted as h, measured with respect to the wing root, positive upward.

Aircraft motion is restricted to be symmetrical with respect to the fuselage centerline.

Three equations are required to describe the symmetrical motion of this aircraft. One equation describes the vertical motion of the aircraft's center of gravity. A second equation describes the motion of the flexible wing, while the third equation describes the pitch motion of the aircraft. These equations were nondimensionalized and then written in matrix form. The form of these equations is as follows:

$$[M_{ij}] \begin{Bmatrix} \ddot{w} \\ \ddot{\bar{h}} \\ \ddot{\theta} \end{Bmatrix} + [K_{ij}] \begin{Bmatrix} w \\ \bar{h} \\ \theta \end{Bmatrix} = \begin{Bmatrix} Q_w \\ Q_{\bar{h}} \\ Q_\theta \end{Bmatrix} \tag{1}$$

The elements of each of the 3x3 matricies in Eqn. 1 are derived in Appendix A. This is done by first forming expressions for the aircraft's kinetic energy, strain energy and generalized forces due to the aerodynamic forces acting on the airplane. Lagrange's equations are then used to generate the equations of motion of the airplane when it is perturbed from its equilibrium flight path by an external disturbance.

The elements of the mass matrix, [M], are real and symmetrical. Pitch and plunge are not coupled dynamically because the coordinates chosen to describe aircraft pitch/plunge motion are located at the aircraft c.g. However, bending motion is inertially coupled together with both pitch and plunge

motion in the mass matrix. Two important nondimensional terms appear in the mass matrix and are defined as follows:

$$\mu = \frac{2ml}{M_F} \tag{2}$$

$$\beta = \frac{M_S}{ml} \tag{3}$$

The elements represent the wing mass to fuselage mass ratio and store mass to wing mass ratios respectively.

The elements of the stiffness matrix [K], are derived from the expression for the strain energy of the wing in terms of h, the tip deflection, and an artificial plunge spring, k.

The generalized forces, Q_w, Q_h and Q_θ, acting on the aircraft wings and canard arise from the distributed airloads along the wings and a single concentrated force on the canard. These loads depend on wing deformation and aircraft attitude and motion. If the aircraft is given an arbitrary virtual displacement, consisting of δw, δh, $\delta\theta$, the virtual work done by the airloads on the wing may be written as follows:

$$\delta W_e = Q_\theta \delta\theta + Q_h \delta h + Q_w \delta w \tag{4}$$

Using Eqn. 4, and the expressions for virtual work (see Appendix A) the expressions for the generalized forces in terms of displacements, w, h and θ can be formulated.

Methods of Solution

The solutions of the time dependent equations of motion are of the form $\{\xi\}e^{st}$. Making this substitution, the equations of motion become:

$$[s^2[M] + [K] + q[A]]\ \{\xi\} = \{0\} \tag{5}$$

Eqn. 5 is an eigenvalue problem with s as the eigenvalue. Matrix [A] is the aerodynamic influence coefficient (AIC) matrix. The AIC's can be divided into real and imaginary parts. They are functions of s also.

For the unsteady aerodynamic representation the AIC's are functions of reduced frequency, k. However, the quasi-steady representations for the AIC's are independent of reduced frequency.

A computer program was developed to calculate the eigenvalues, s, for the system of equations. To find the eigenvalues, the equations of motion were put into the following form:

$$[A]\{X\} = s\{X\} \tag{6}$$

In Eqn. 5, s is the eigenvalue and $\{X\}$ is a vector of displacements and velocities of the system. To convert the problem from that given in Eqn. 5 to that shown in Eqn. 6, consider the following.

The equations of motion for this system can be written as:

$$[M]\{\ddot{q}\} + [B]\{\dot{q}\} + [K]\{q\} = \{0\} \tag{7}$$

A new variable, $\bar{q}$, is now introduced to reduce this second order system, Eqn. 7, into a first order system.

$$\{\bar{q}\} = s\{q\} \tag{8}$$

Substitute Eqn. 8 into Eqn. 7. The resulting equation is:

$$s[M]\{\dot{q}\} + [B]\{\dot{q}\} + [K]\{q\} = \{0\} \tag{9}$$

Rewriting Eqn. 9 we get:

$$-[M]^{-1}[B]\{\dot{q}\} - [M]^{-1}[K]\{q\} = s\{\dot{q}\} \tag{10}$$

Eqn. 8 can be rewritten as:

$$[I]\{\dot{q}\} = sq \tag{11}$$

Combining Eqns. 10 and 11, the equations of motion can be put into the form shown in Eqn. 6. In this case:

$$[A] = \begin{bmatrix} [0] & [I] \\ -[M]^{-1}[K] & -[M]^{-1}[B] \end{bmatrix} \tag{12}$$

and

$$\{X\} = \begin{Bmatrix} q \\ \dot{q} \end{Bmatrix} \tag{13}$$

Matrix [A] is a 6x6 matrix. There are six roots to this equation. They may be either complex conjugates or real. The complex conjugate eigenvalues are of the form:

$$s = \sigma \pm i\omega \tag{14}$$

Where σ represents the system damping and ω is the frequency of oscillation.

These roots may be plotted in a "root locus" format using σ and $j\omega$ as coordinates. The roots with negative frequencies are omitted from these root

locus plots since they are merely reflections of the other complex conjugate roots. However the roots with a zero frequency are of interest. The root locus plot is a valuable tool for determining system stability. Thus stability can be studied by examining the behavior of roots in the "s-plane". Instabilities occur for values of damping, σ, greater than or equal to zero.

Two solution techniques were used to solve the flutter problem. The first, using an unsteady representation of the aerodynamic forces, is called the P-K method. The other method is a variation of P-K method using quasi-steady aerodynamics. A detailed description of these methods is given in Appendix B.

Several aircraft parameters are to be varied. These parameters are the wing position, $\bar{x}$, wing tip store position, $\bar{x}_s$, and the store to wing mass ratio, β. Several different situations were considered and are listed in Table 3. To begin with, the stability of the aircraft without tip stores was studied. These so-called "clean wing" cases are compared to the cases with stores to determine the effects the addition of the wing tip stores have on the stability of the system. Also, calculations were made using quasi-steady and unsteady aerodynamics for identical geometrical and inertial input parameters. A comparison of the results obtained from these aerodynamic formulations will be made to determine differences in the calculated flutter speed of the aircraft.

Table 3 Clean Wing and Wing/Store Cases

	Case No.	$\bar{x}_z$	β	Store Loc.	Quasi-Steady	Unsteady
	1	0.50				x
	2	0.50				
	3	0.45			x	
	4	0.45				x
Clean	5	0.40			x	
Wing	6	0.40				x
	7	0.35			x	
	8	0.35				x
	9	0.30			x	
	10	0.30				x
	11-15	0.50	0.30	0-c	x	
Wing	16-20	0.50	0.30	0-c		x
with	21-25	0.40	0.30	0-c	x	
Store	26-30	0.40	0.30	0-c		x
	31-35	0.30	0.30	0-c	x	
	36-40	0.30	0.30	0-c		x
	41	0.30	0.30	0	x	
	42	0.30	0.60	0	x	

*Stores were varied from leading edge, 0, to trailing edge, c, at 1/4 c increments.

RESULTS AND DISCUSSION

The first case we will consider is an aerodynamically stable wing/body/canard combination without tip stores. This airplane has a 30° forward swept wing, $\mu = 0.11$, and a cantilever wing flexural frequency $\omega_0 = 68$rad/sec. The wing root fuselage junction is aft of the aircraft c.g. at the position $\bar{x} = 0.35$. (see Figure 1). Note that the barred quantities, such as $\bar{x}$, refer to a parameter that is divided by the wing semi span, l.

Figure 3 shows a root locus plot of the eigenvalues for a quasi-steady aerodynamic analysis of this configuration as airspeed, V, increases. Each point on the plot corresponds to a different airspeed. These values for airspeed are shown nondimensionalized with respect to a reference speed, V_{DC}, the airspeed at which the clamped wing encounters aeroelastic divergence.

Two curves are plotted in Figure 3. The first represents the behavior of the pitch mode (also called the *short period mode)* as V/V_{DC} increases. The frequency of the pitch mode first increases while pitch damping also increases. However, near $V/V_{DC} = 0.90$, frequency begins to decrease until the root locus plot intersects the real axis. At this point, the root divides and moves along the real axis.

The coupled bending mode decreases in frequency and increases in damping, σ, until a velocity near $V/V_{DC} = 0.80$. The bending root then moves toward the right half plane as airspeed increases. At $V_F/V_{DC} = 0.949$, the bending mode becomes unstable. Aeroelastic coupling, involving the two

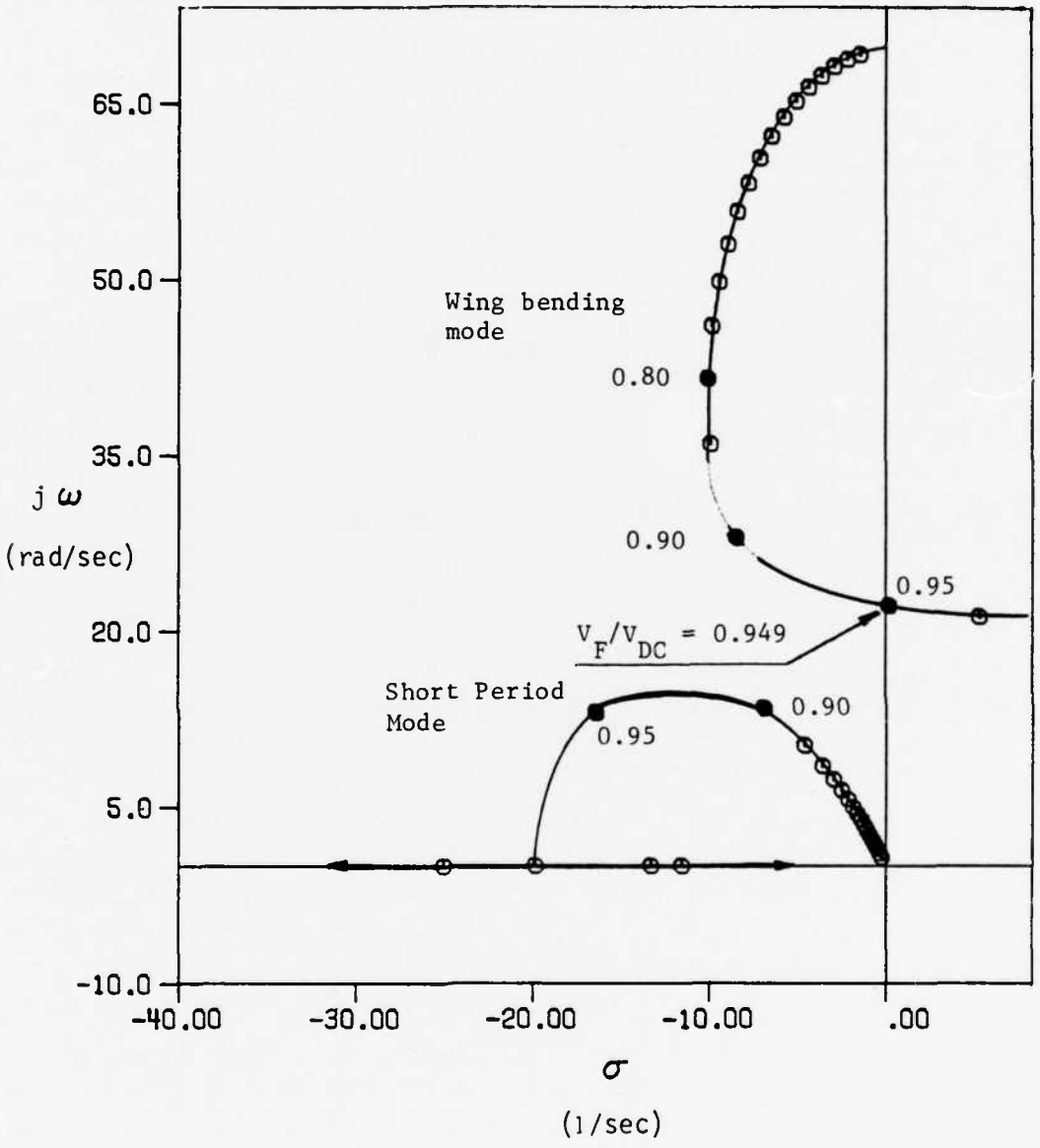

Figure 3 Root Locus Plot for $\bar{x} = 0.35$, Quasi-Steady Aerodynamic Theory

rigid-body freedoms and the single bending mode, leads to a dynamic instability of the airplane referred to as body-freedom flutter (3). Although the traditional scheme for identifying aeroelastic modes (bending, pitch) has been used here, these are not normal modes. In fact they each contain large amounts of bending, plunge and pitch.

One other root is present in the analysis, but is not shown. This root involves the plunge mode and is located at and near the origin along the σ axis. Since this root is of no significance to the aeroelastic stability analysis, it is omitted from the root locus plots to follow.

Figure 4 is a root locus plot for the same aircraft configuration. However unsteady aerodynamic theory is used to model the aerodynamic forces. In this figure the coupled bending mode is well damped at all airspeeds. The coupled pitch mode frequency, ω, and damping, σ, increase with increasing airspeed until a velocity slightly above $V/V_{DC} = 0.85$. The pitch root then moves toward the right half of the s-plane as airspeed increases. At $V_F/V_{DC} = 0.96$ the pitch mode becomes unstable at a frequency of 18.21 rad/sec and a reduced frequency $k = 0.0203$.

The most noteworthy difference between these two root locus plots, Figures 3 and 4, is the apparent change in the origin of the flutter mode. The the flutter speed, as calculated from the quasi-steady representation, is slightly lower than the flutter speed calculated with the unsteady aerodynamic representation, (see Figure 4). However, although the ancestry of the flutter mode is different, the coupled instability mode is nearly the same in both cases.

The next case considered is an unstable wing/body combination. This airplane is identical to the one given in the previous discussion, except that the wing root position is moved closer to the aircraft c.g. to a position $\bar{x} = 0.30$.

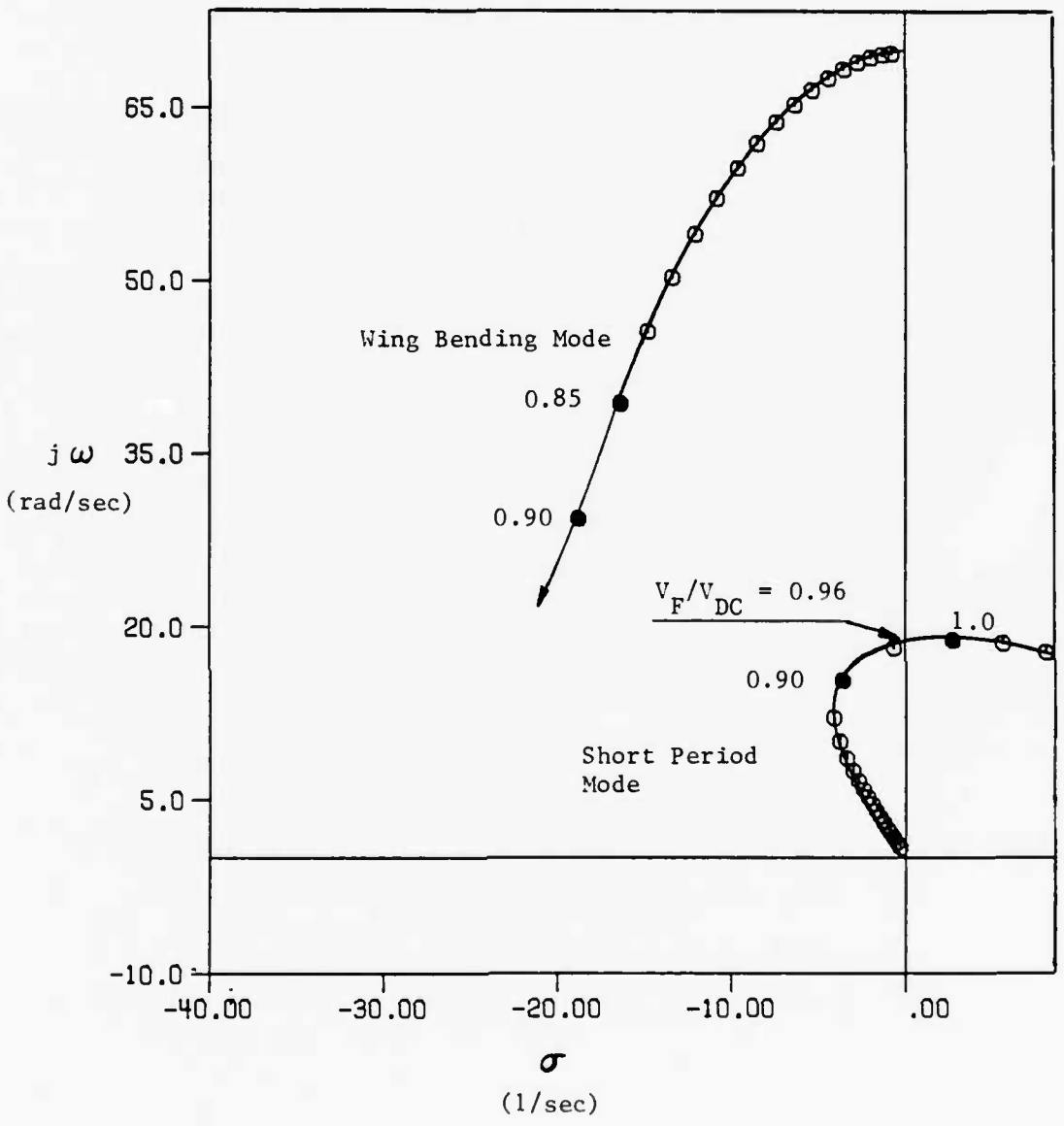

Figure 4 Root Locus Plot for $\bar{x} = 0.35$, Unsteady Aerodynamic Theory

As before two root-locus plots are of interest.

Figure 5 is a root locus plot for this configuration using a quasi-steady representation for the aerodynamic loads. The coupled wing bending mode damping increases while frequency decreases with airspeed until about $V/V_{DC} = 0.80$. The bending root then moves toward the right half plane as airspeed increases. At $V_F/V_{DC} = 1.003$ the wing bending mode becomes unstable. For the coupled pitch mode the roots are non-oscillatory. Some of these roots pass into the right half plane. This indicates a "static" or aperiodic instability in the pitch mode. To further illustrate this instability, Figure 6 shows damping, σ, vs. non-dimensional velocity, V/V_{DC} for each mode. This figure, like the root-locus, indicates an instability when values for σ are greater than zero. As seen in Figure 6, there are two coupled pitch modes, one stable, the other unstable. This figure also shows the bending mode root crossing the zero damping line, indicating the onset of flutter, and the unstable pitch root re-stabilizing in the same vicinity.

Figure 7 is a root locus plot for this same aircraft configuration using classical Theodorsen unsteady aerodynamic theory to model the aerodynamic forces. As before, the coupled wing bending root damping increases and frequency decreases with airspeed until near $V/V_{DC} = 0.90$. This root then moves toward the right half plane as airspeed increases. At $V_F/V_{DC} = 1.033$ the wing bending root becomes unstable. This flutter speed is slightly greater than that obtained from using quasi-steady aerodynamics. The most significant difference between Figures 5 and 6 is seen in the pitch mode. In Figure 5 the pitch mode was non-oscillatory and statically unstable at a low airspeed. However, when using unsteady aerodynamics, the pitch mode becomes oscillatory and the static instability disappears.

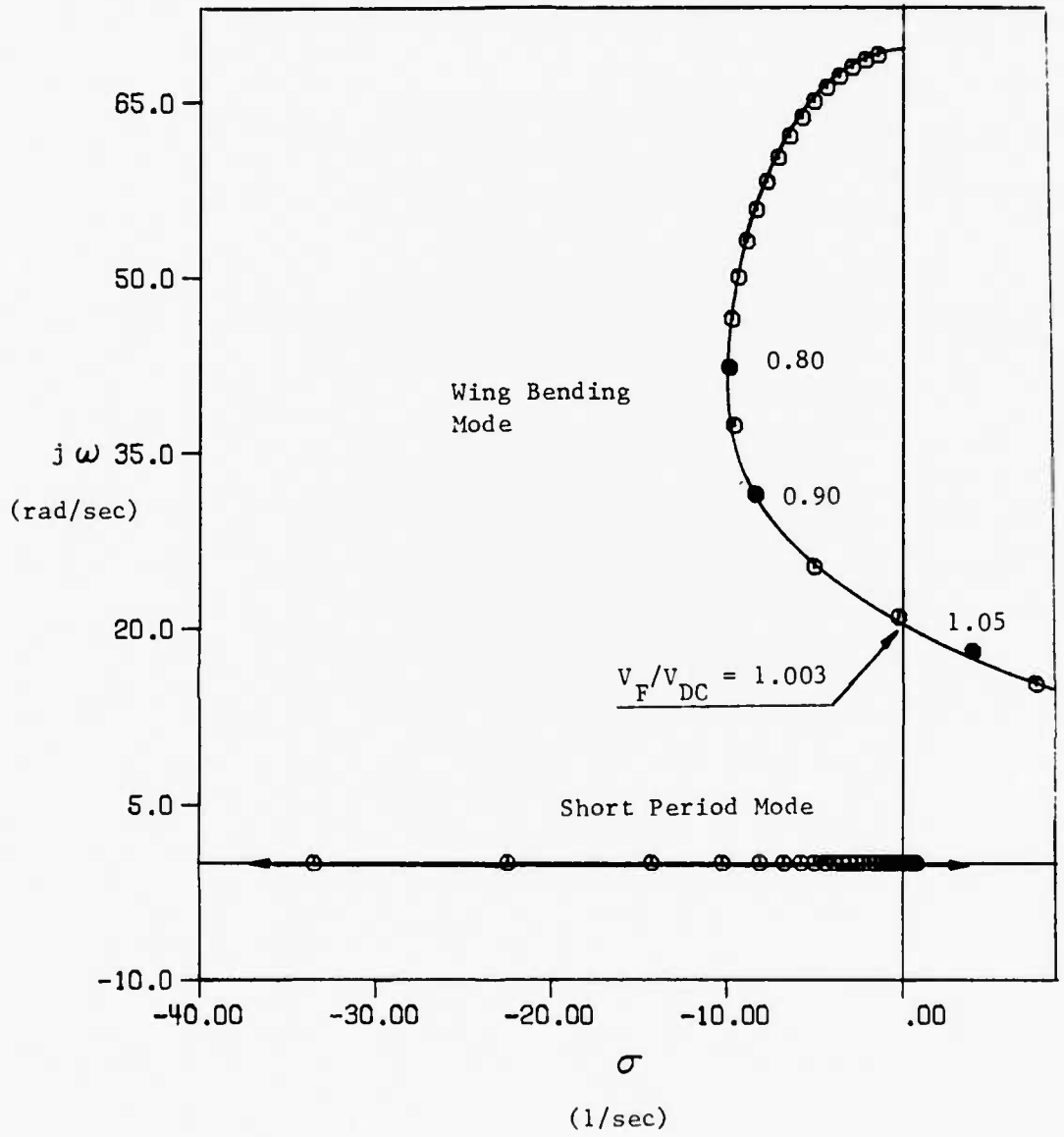

Figure 5 Root Locus Plot for $\bar{x} = 0.30$, Quasi-Steady Aerodynamic Theory

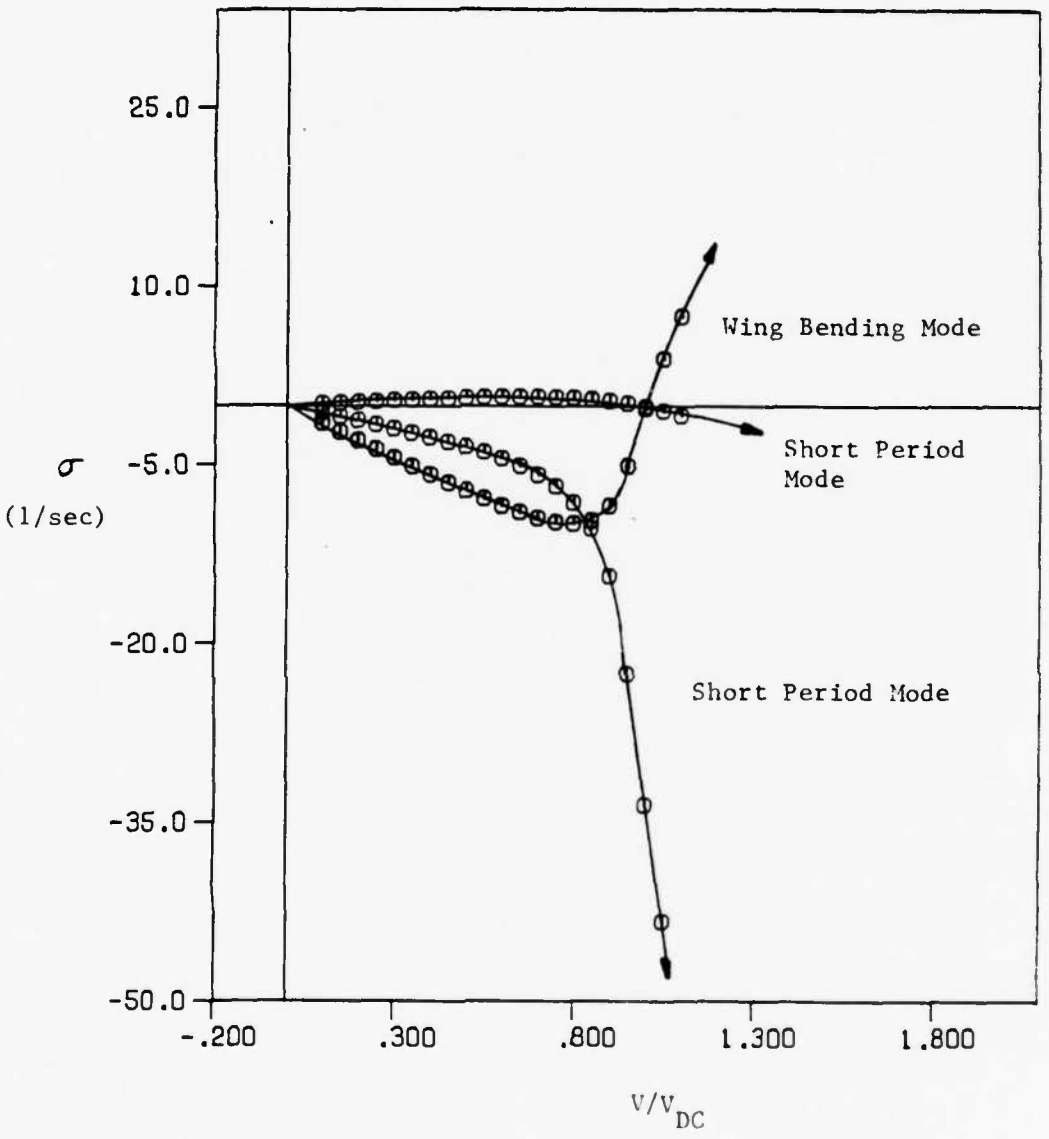

Figure 6 Modal Damping vs. Velocity Ratio when $\pi = 0.30$, Quasi-Steady Aerodynamic Theory

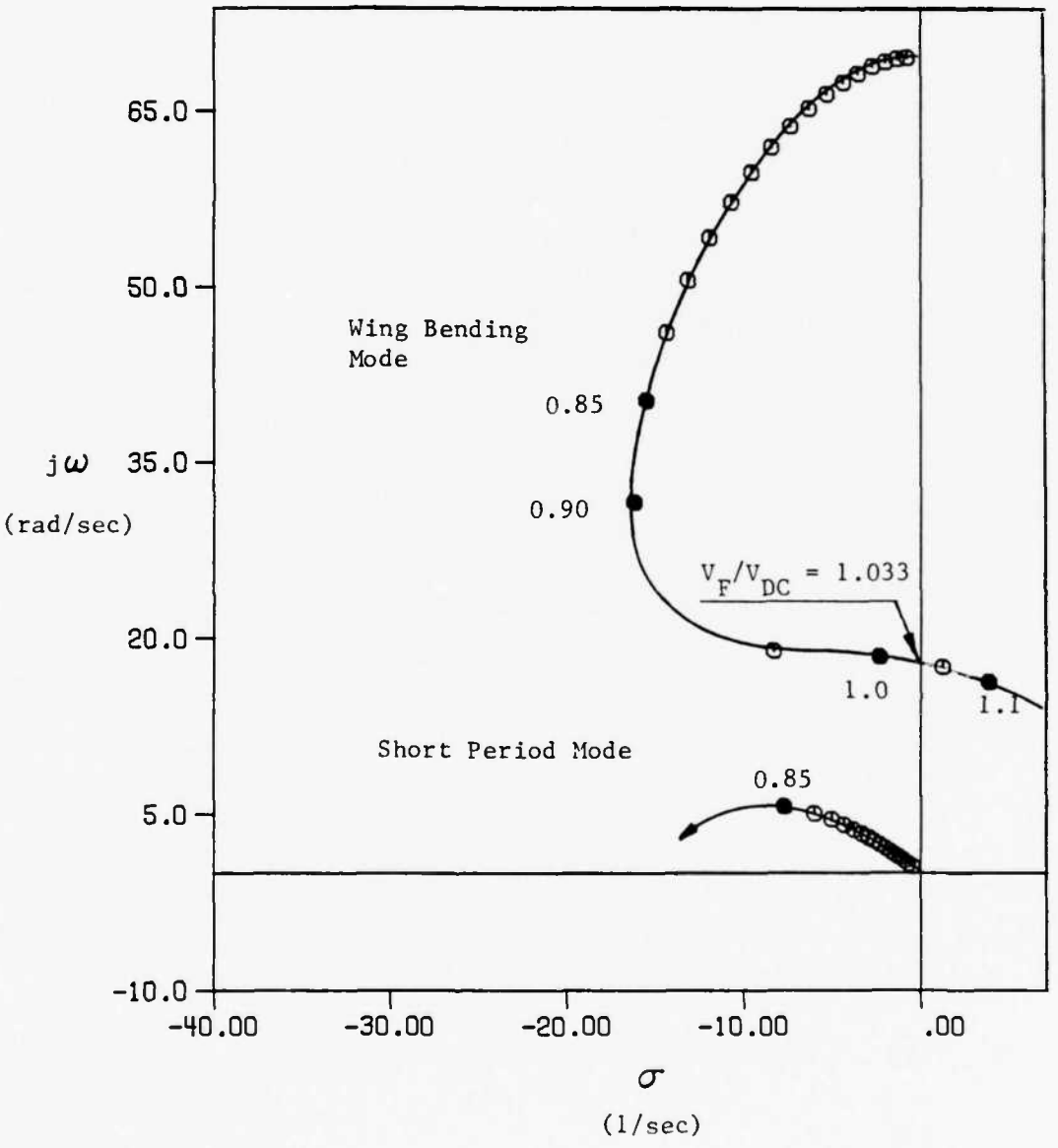

Figure 7 Root Locus Plot for $\bar{x} = 0.30$, Unsteady Aerodynamic Theory

Another indication of differences resulting from the quasi-steady and unsteady aerodynamic formulations is seen by examining a plot of the aircraft flutter speed as the wing position, $\bar{x}$, changes. As shown in Figure 8, the flutter speeds as predicted by quasi-steady and the unsteady aerodynamic theory intersect each other near $\bar{x} = 0.37$. This indicates that the quasi-steady aerodynamic formulation does not always give a larger value for the flutter speed.

When stores are added to the wing tips of the aircraft, very little change in the root locus plots was observed as the store c.g. location, $\bar{x}_s$, was moved fore and aft along the chord of the wing. Figure 9 is a root locus plot for a wing position, $\bar{x}$, of 0.40, store to wing mass ratio, β, of 0.30 and the store location on the wing tip, $\bar{x}_s$, of 0.0, the mid-chord position. Quasi-steady aerodynamics were used to model the aerodynamic forces. Flutter occurs in the coupled wing bending mode.

Figure 10 is a root locus plot for the identical aircraft using an unsteady aerodynamic representation of the aerodynamic forces. In this figure, flutter occurs in the coupled pitch mode. Figures 11, 12, and 13 are plots of flutter speed vs. store position. In each of these figures the quasi-steady flutter speed decreases as the store is moved from leading edge (L.E.) to trailing edge (T.E.). In Figures 11 and 12 the flutter speed found with the unsteady aerodynamic representation increases as the store is moved from L.E. to T.E. This trend is opposite to that seen with the quasi-steady aerodynamic representation. Also, as was seen for the clean wing cases, quasi-steady aerodynamics does not always give a lesser value for the flutter speed. In Figure 11, the quasi-steady flutter speed is higher than the unsteady flutter speed, but in Figures 12 and 13 the opposite is true.

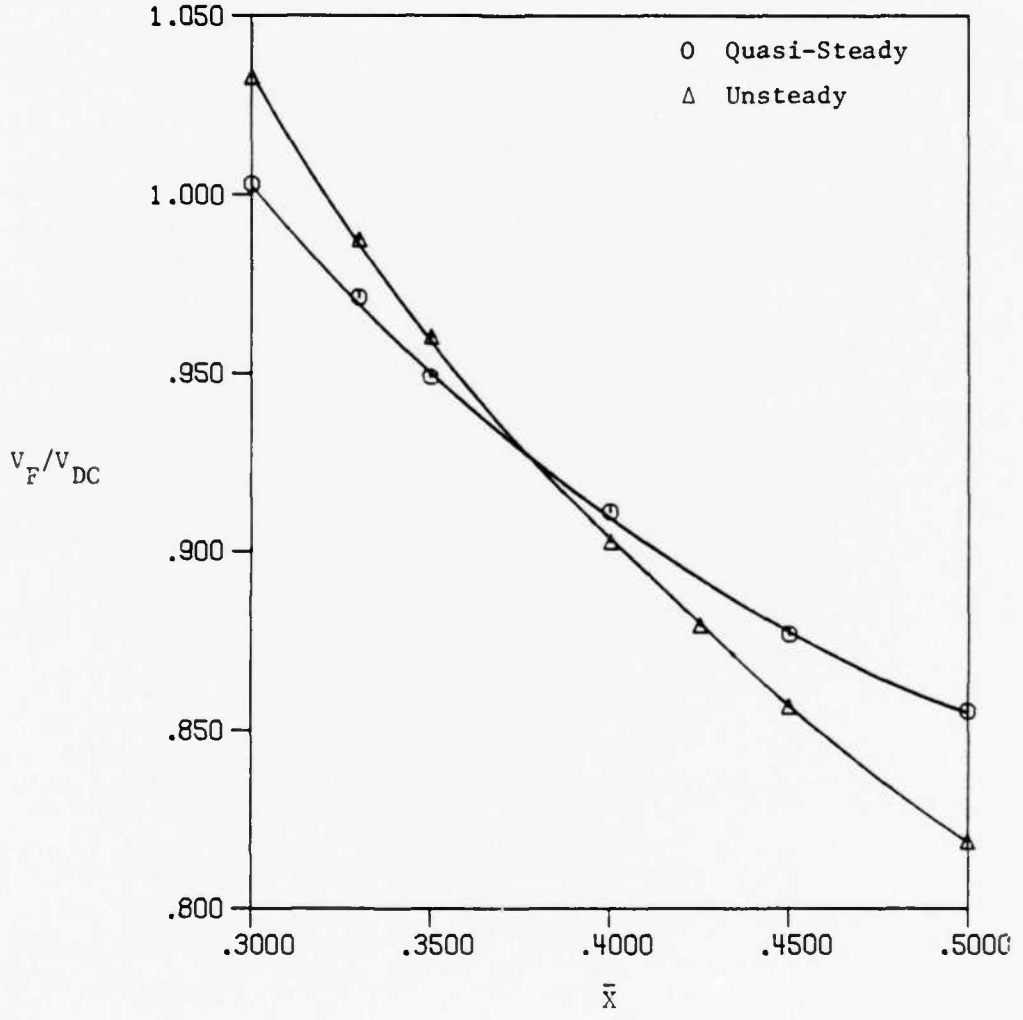

Figure 8 A Comparison of Flutter Speed Ratios (V_F/V_{DC}) vs. Wing Position ($\bar{x}$), with Quasi-Steady and Unsteady Aerodynamic Theories

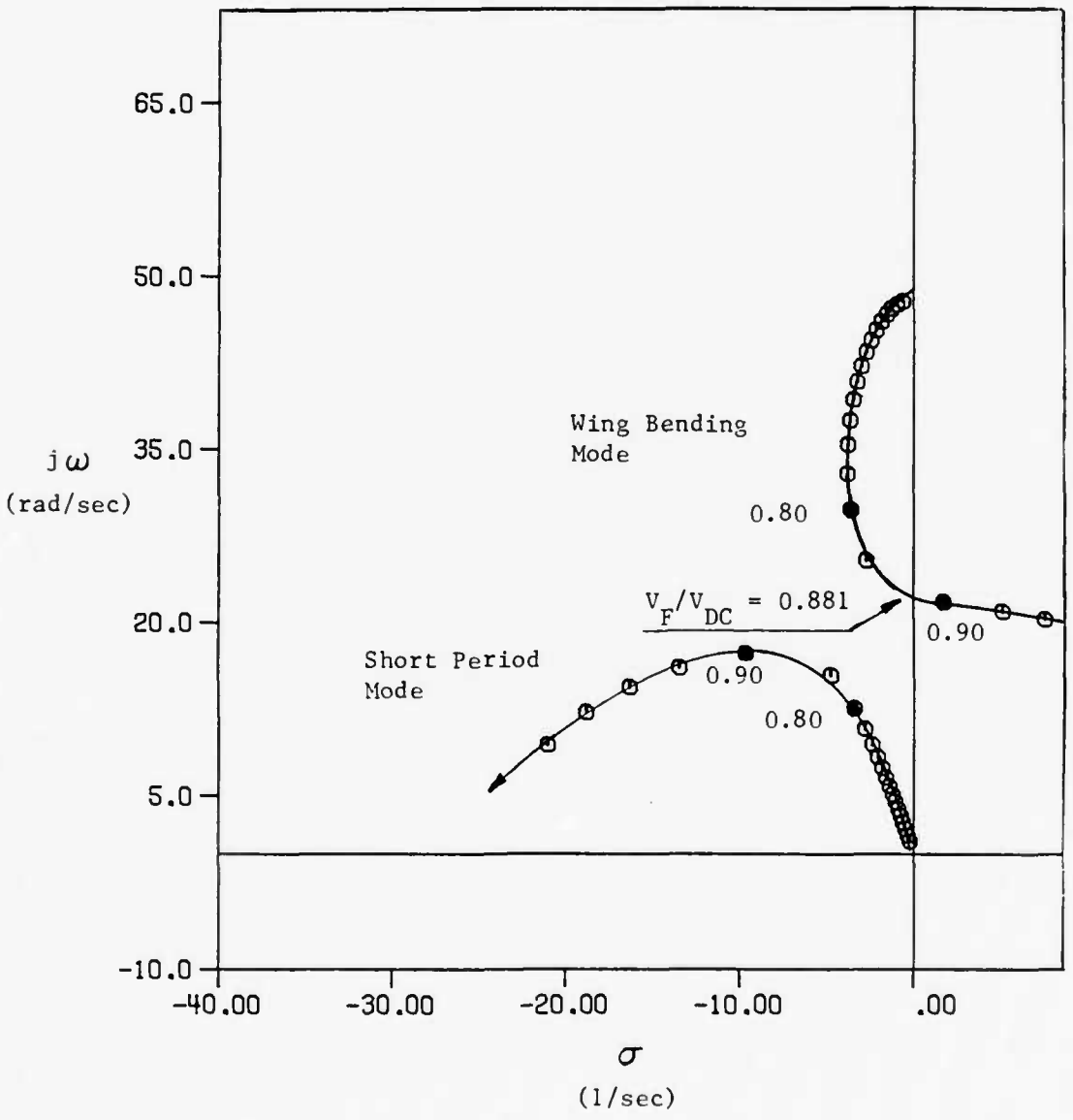

Figure 9 Root Locus Plot for $\bar{x} = 0.40$, Quasi-Steady Aerodynamic Theory, with Store c.g. at Wing Midchord ($\bar{x}_s = 0$)

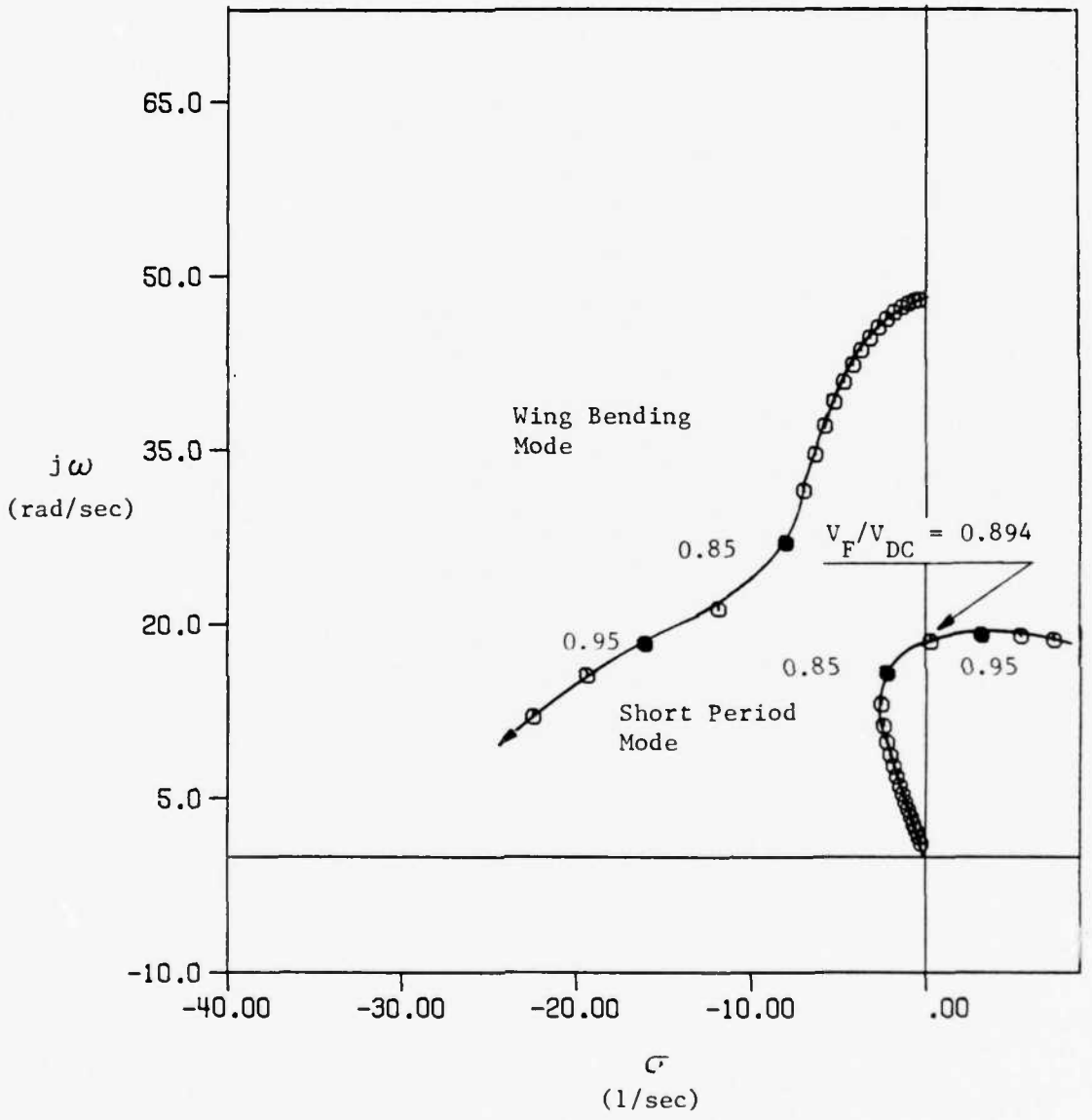

Figure 10 Root Locus Plot for $\bar{x} = 0.40$, Unsteady Aerodynamic Theory, with Store c.g. at Wing Midchord ($\bar{x}_s = 0$)

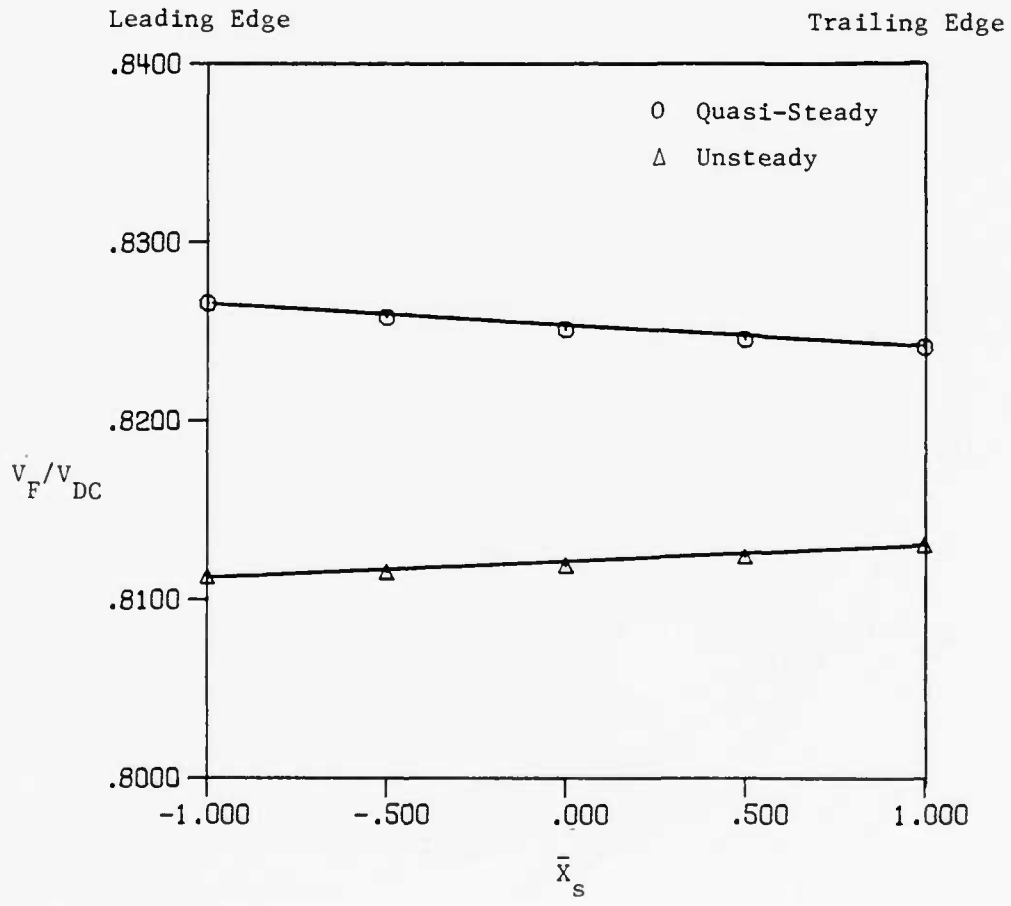

Figure 11 Flutter Speed Ratio vs. Tip Store c.g. Position for $\bar{x} = 0.50$

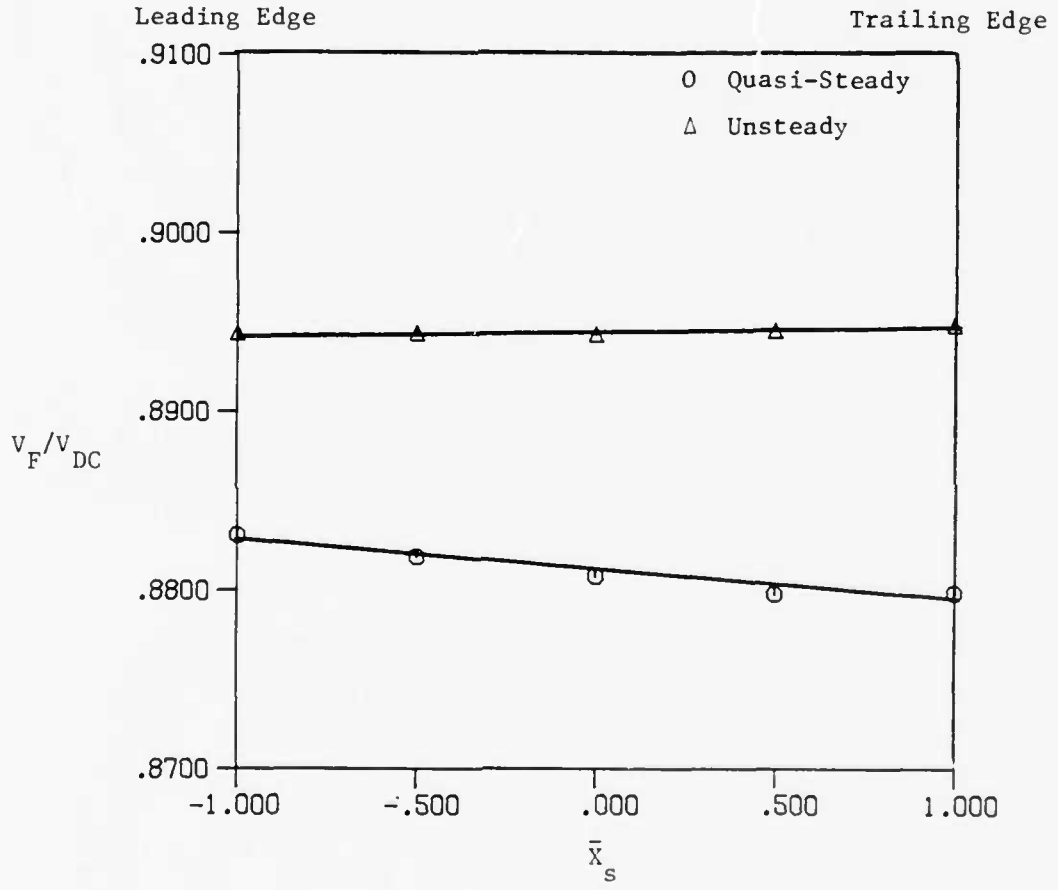

Figure 12 Flutter Speed Ratio vs. Tip Store c.g. Position for $\bar{x} = 0.40$

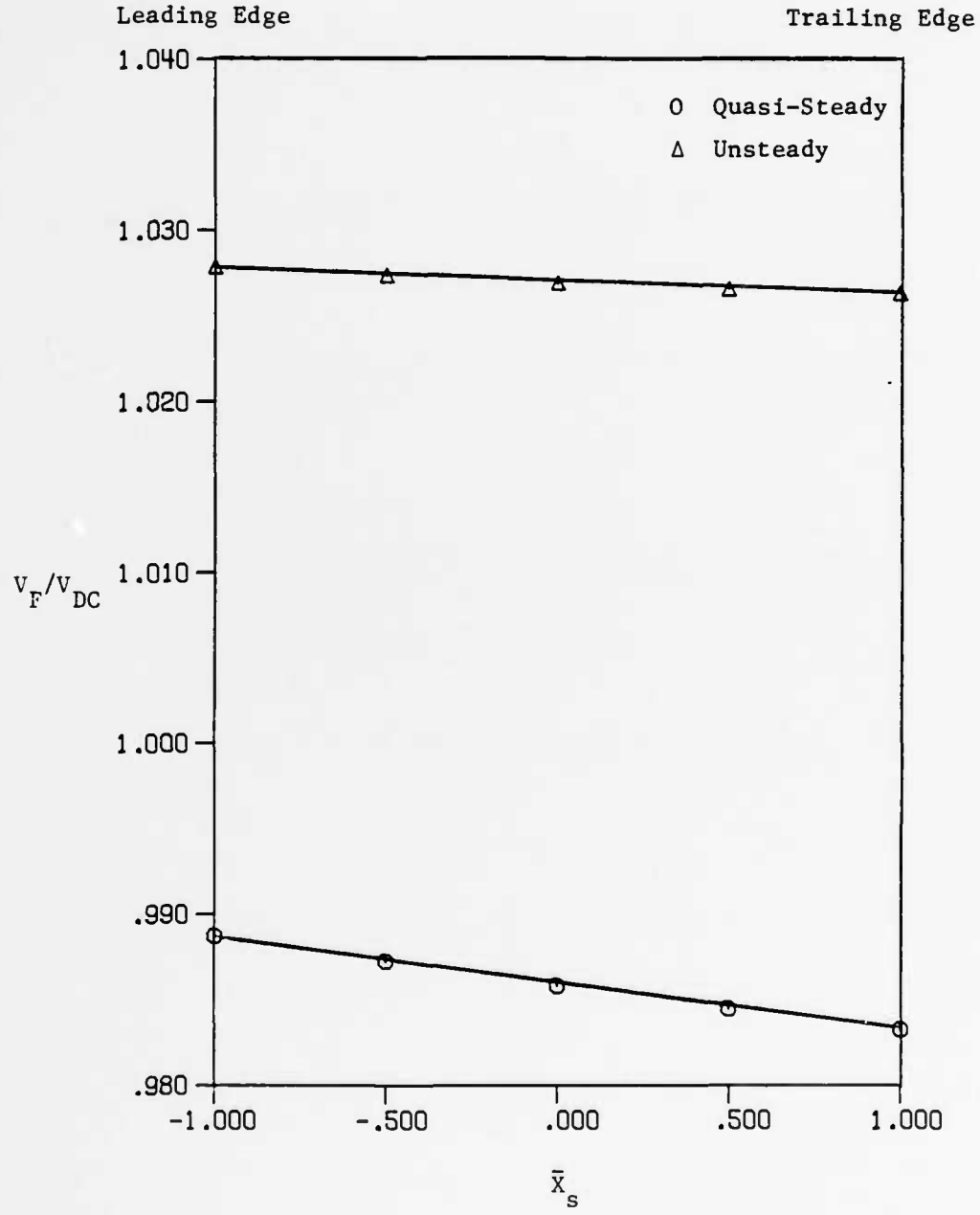

Figure 13 Flutter Speed Ratio vs. Tip Store c.g. Position for $\bar{x} = 0.30$

Another interesting difference between the results obtained with the two aerodynamic formulations is found from a comparison of the clean wing flutter speeds with the flutter speeds obtained with wing tip stores. Figures 14 and 15 are plots of flutter speed, V_F/V_{DC} vs. wing position, $\bar{x}$, for the clean wing cases and for the cases with a store located on the midchord. In these figures, it is evident that the flutter speed decreases when stores are added to a clean wing. Figure 14, for quasi-steady aerodynamics, shows that, as the wing moves aft of the aircraft c.g., the differences between the flutter speeds of the clean wing and the wing with a tip store increase. However, with unsteady aerodynamics, Figure 15 shows that the difference between the flutter speeds remains relatively constant.

It was noted earlier in this study that the use of different aerodynamic theories to represent the aerodynamic forces of the aircraft model changed the flutter mode. This flutter mode change also occurs when wing tip stores are added. Figure 9 is a root locus plot for $\bar{x} = 0.40$, $\beta = 0.30$ and $\bar{x}_s = 0$. Flutter, for this aircraft geometry, occurred in the coupled wing bending mode. Figure 16 is a root-locus plot for the same aircraft configuration. with the store removed. Flutter now occurs in the coupled pitch mode.

For a forward swept wing, a situation could arise such that the wing center of pressure lies ahead of the aircraft c.g. For an aircraft with a canard, this configuration will be statically unstable. Figure 5 is an example of a root locus plot for such a configuration. Figure 17 is a root locus plot for the same aircraft configuration but with the addition of a tip store on the leading edge of the wing. The aircraft parameters are $\beta = 0.30$, and $\bar{x} = 0.30$. Quasi-steady aerodynamics were used for these results. Note that with the addition of the store, this configuration is no longer statically unstable because the aircraft c.g.

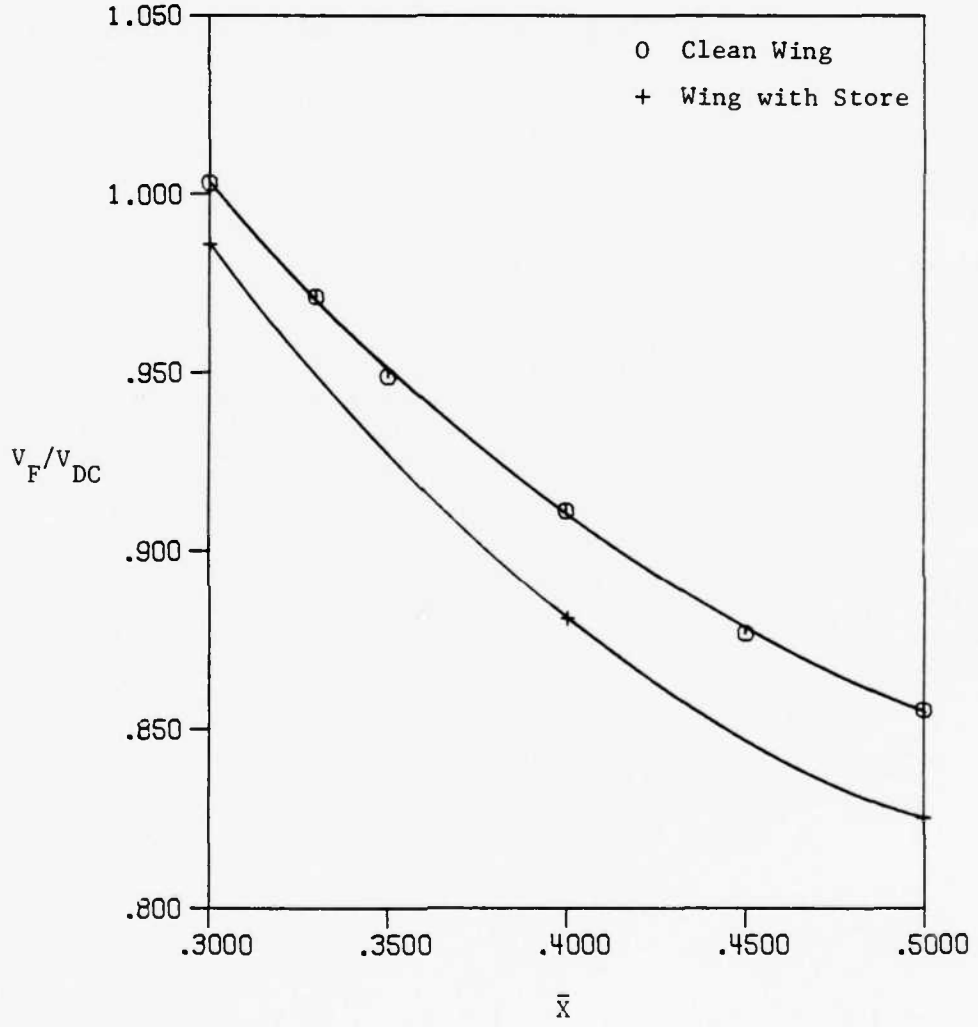

Figure 14 Flutter Speed Ratio vs. Wing Position with and without Stores Placed at the Midchord, Quasi-Steady Aerodynamic Theory

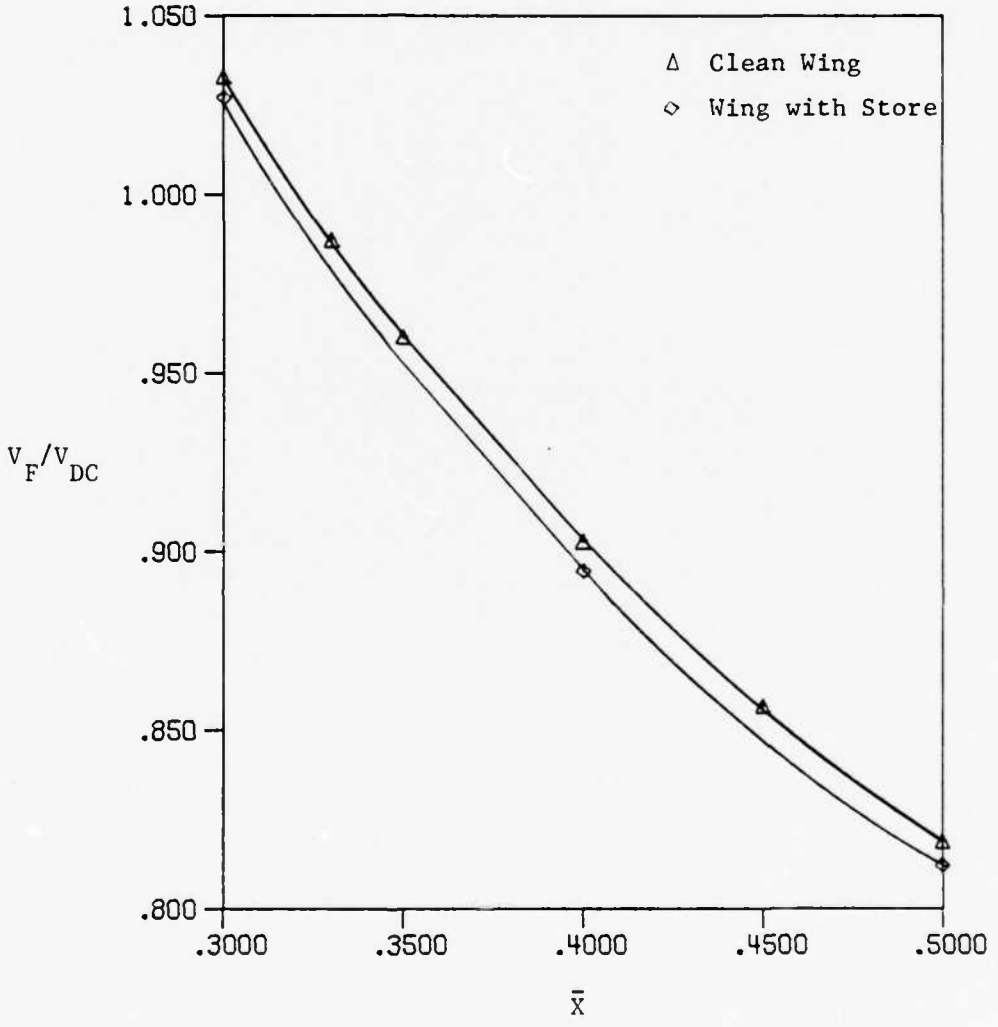

Figure 15 Flutter Speed Ratio vs. Wing Position with and without Stores at Midchord, Unsteady Aerodynamic Theory

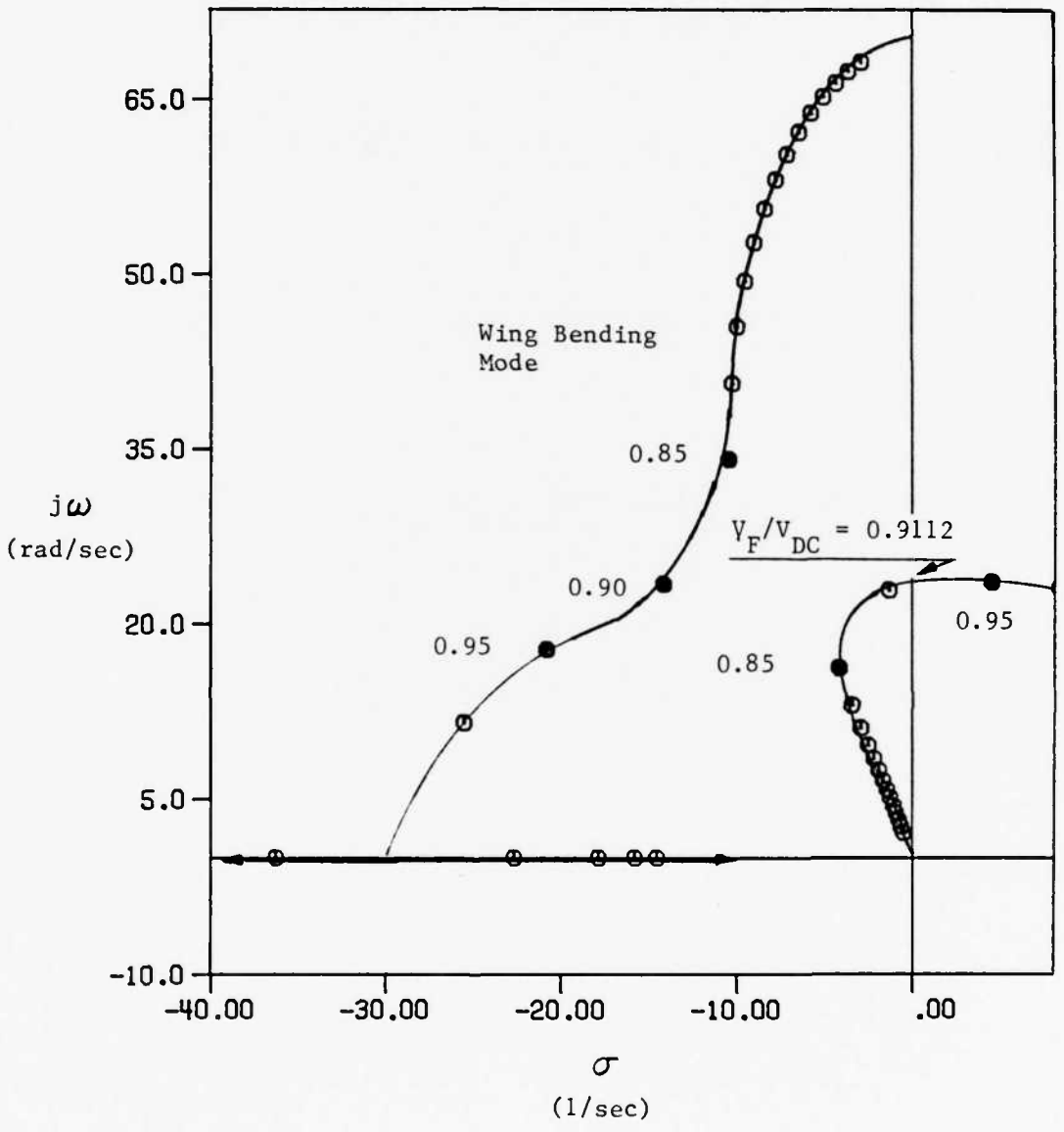

Figure 16 Root Locus Plot for $\bar{x}$ = 0.40 Quasi-Steady Aerodynamic Theory Clean-Wing

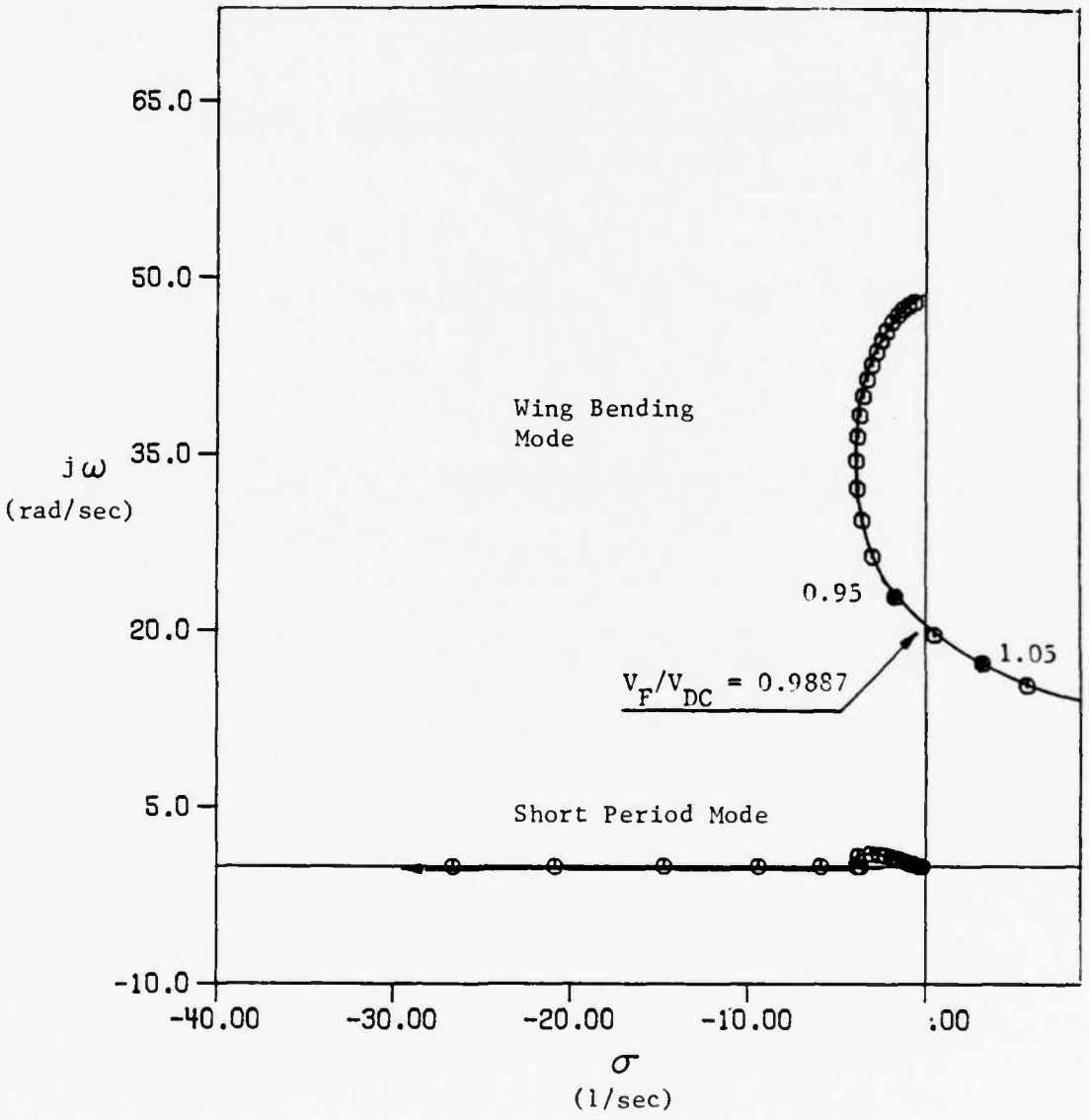

Figure 17 Root Locus Plot for $\bar{x} = 0.30$, $\beta = 0.30$, Quasi-Steady Aerodynamic Theory with Store c.g. at Leading Edge

has been moved forward by the addition of the store on the wing tip. In fact, the pitch mode went from non-oscillatory to slightly oscillatory. Also the flutter speed was reduced from $V_F/V_{DC} = 1.003$ without a store to $V_F/V_{DC} = 0.98872$ with the store. To further illustrate this finding, another root locus plot was generated for the same aircraft parameters as the previous case. However, the store/wing mass ratio, β has been doubled. Figure 18 is a root locus plot for $\bar{x} = 0.30$ and $\beta = 0.60$. Again quasi-steady aerodynamics were used. Note the increase in frequency for the pitch mode. Again, as before, the addition of the wing tip store has further reduced the flutter speed from $V_F/V_{DC} = 0.989$ to $V_F/V_{DC} = 0.978$. With the addition of the store on the wing tip, the aircraft c.g. moved sufficiently forward ahead of the wing center of pressure to eliminate the static instability.

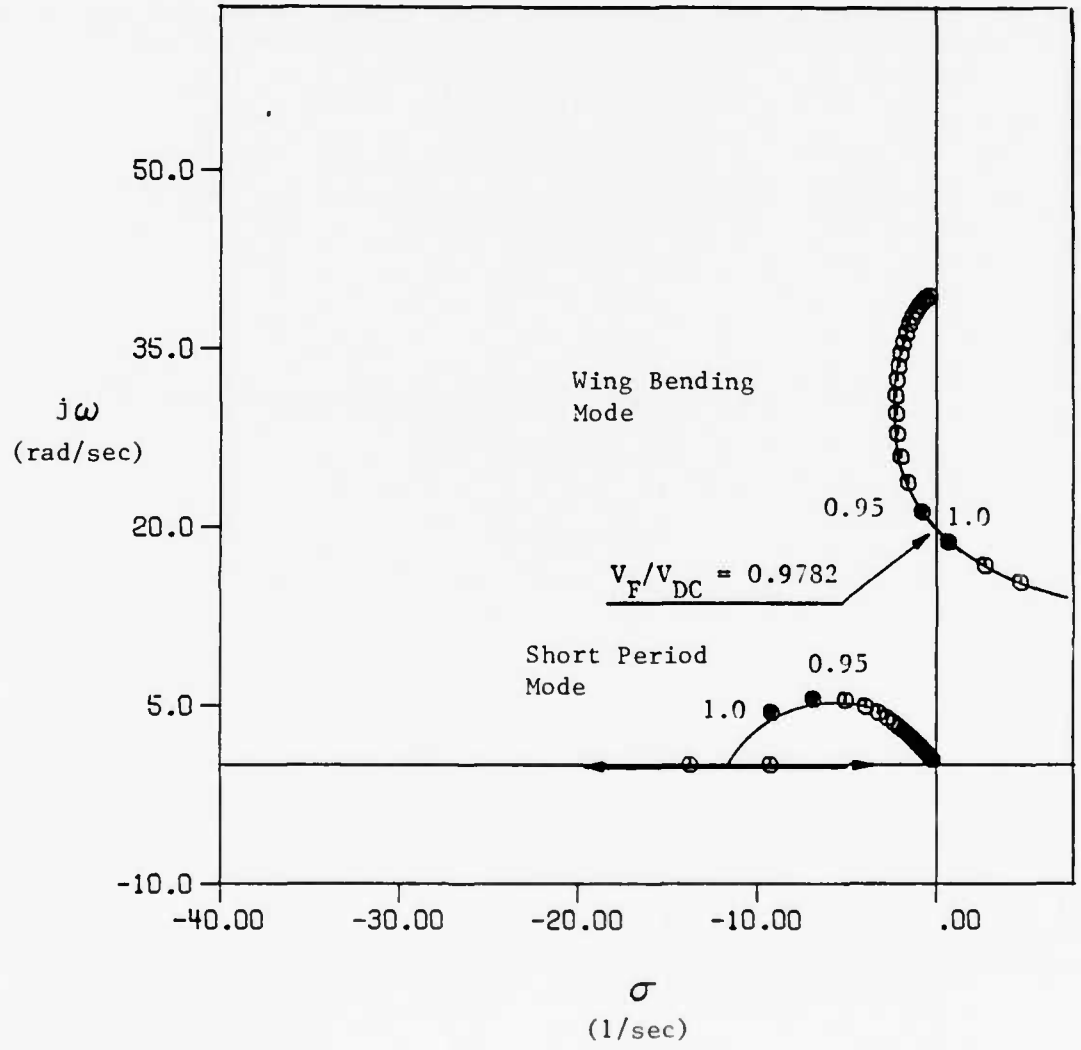

Figure 18 Root Locus Plot for $\bar{x} = 0.30$, $\beta = 0.60$, Quasi-Steady Aerodynamic Theory with Store c.g. at Leading Edge

SUMMARY AND CONCLUSIONS

One of the purposes of this study was to identify potential differences in the stability characteristics of an idealized forward swept wing aircraft model when quasi-steady and unsteady aerodynamic formulations are used. Also, the effect of the inclusion of wing tip stores on the stability of the forward swept wing aircraft model was considered. Because of the simplicity of the model and the limited number of cases analyzed, general conclusions relevant to all forward swept wing aircraft cannot be made. However, from these preliminary studies, some conclusions can be drawn.

Several differences were noted in the stability characteristics of the aircraft model, depending upon whether or not quasi-steady or unsteady aerodynamic theory was used. Flutter occurred in a different mode depending on the aerodynamic formulation used. A statically unstable aircraft configuration using quasi-steady aerodynamics was found to be stable when unsteady aerodynamics were used. It was also shown that quasi-steady aerodynamics does not always give lower values for the flutter speed than does the unsteady aerodynamic representation.

When an aeroelastic stability analysis is performed on an aircraft, it is necessary to consider all the aircraft modes to determine precisely which mode caused the instability. Also, because of the differences in the stability characteristics encountered when using the quasi-steady and unsteady

formulations for the aerodynamic loads, an accurate representation of these loads is essential.

When stores were added to the wing tip, the flutter speed generally decreased for quasi-steady aerodynamics as the store was moved from leading edge to trailing edge. However, for one of the wing positions studied this trend was reversed when unsteady aerodynamics were used. It was also found that, with quasi-steady aerodynamics, the differences between the flutter speeds for the clean wing and the wing with stores increased as the wing was moved aft of the A/C c.g., while, with unsteady aerodynamics the differences between the flutter speeds remained relatively constant. Also, when stores are added to the wing tip of a statically unstable FSW aircraft geometry, it was found that this instability disappeared. Generally, however, it was found that the flutter speed was lower when stores were added to the wing tips regardless of the aerodynamic representation used for this study.

LIST OF REFERENCES

LIST OF REFERENCES

1. Krone, N.J., Jr., "Divergence Elimination with Advanced Composites", AIAA Paper No. 75-1009, Aug. 1975.

2. Swaim, R.L., "Launch Vehicle Mode Interaction", *AIAA Journal*, Vol. 6, No. 4, pp. 753, 754, Nov. 1967.

3. Weisshaar, T.A., and Zeiler, T.A., "Dynamic Stability of Flexible Forward Swept Wing Aircraft", AIAA Paper 82-1325, August 1982.

4. Bisplinghoff, R.L., Ashley, H., and Halfman, R.L., *Aeroelasticiy*, Addison-Wesley, 1955.

5. Fung, Y,C., *The Theory of Aeroelasticity*, Dover, 1975.

6. Schwendler, R.G., and MacNeal, R.H., "Optimum Structural Representation in Aeroelastic Analyses", Air Force Flight Control Laboratory, Report No. ASD-TR-61-680, March 1962.

APPENDICES

APPENDIX A

Development of Perturbed Equilibrium Equations With the Addition of Wing Tip Stores

This appendix presents the development of the equations of motion for a three degree-of-freedom forward swept wing model with wing tip stores. A planform view of this model is shown in Figure A-1. The degrees-of-freedom are: w, aircraft plunge; θ, aircraft pitch attitude; and, h, wing bending or flexure.

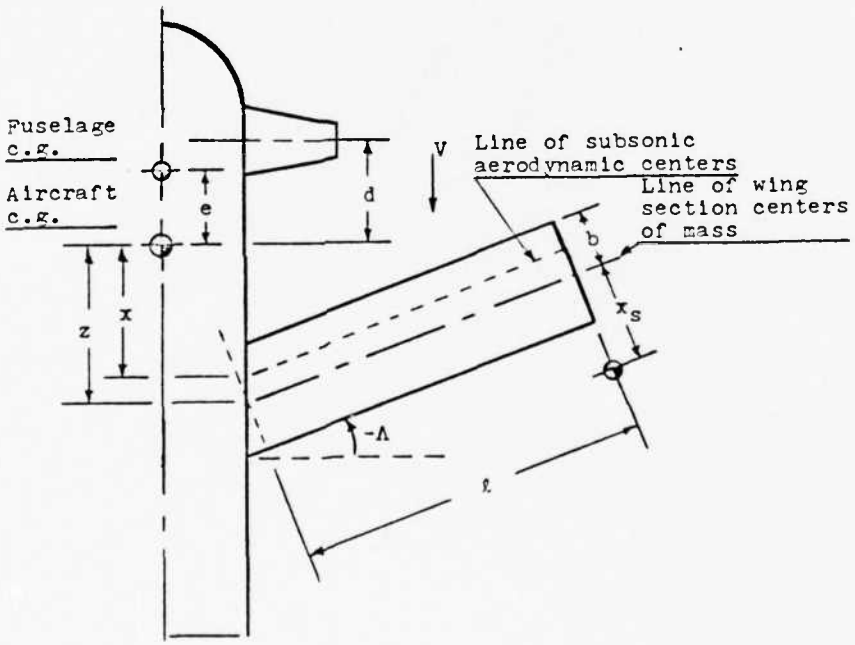

Figure A-1 Planform Geometry and Nomenclature

The equations of motion are developed by using Lagrange's equations, together with an assumed deflection shape for wing bending vibration. Expressions for the kinetic energy, T, the strain energy, U, and expressions for

the generalized aerodynamic forces associated with each degree of freedom, will be formulated.

The kinetic energy of the aircraft and stores is written as:

$$T = \frac{1}{2}\left[M_F\,(\dot{w} + e\dot{\theta})^2 + I_F\,\dot{\theta}^2\right] \tag{A-1}$$

$$+ 2\left(\frac{1}{2}\right)\int_o^l\int_c \rho[\dot{w} - (z + y\sin\Lambda + \xi\cos\Lambda)\dot{\theta} + \dot{h}]^2 d\xi dy$$

$$+ \frac{1}{2}\,(2M_S)\,\dot{h}_s^2 + \frac{1}{2}\,(2I_S)\,\dot{\theta}^2$$

The first bracketed term Eqn. A-1 represents the kinetic energy of the fuselage; the integral term accounts for the kinetic energy of the mass distributed over the wing surface area S. The last two terms represent the kinetic energy of the wing tip stores. The coordinates (y,ξ) define the location of a mass point on the wing with respect to the wing root origin located a distance z, aft of the aircraft c.g. The vertical velocity of the store c.g., $\dot{h}_s$, is given by the expression:

$$\dot{h}_s = \dot{w} + \dot{h} - (z + l\sin\Lambda + x_s)\dot{\theta} \tag{A-2}$$

This analysis will be restricted to a uniform planform wing with constant mass per unit area distributed uniformly about the y-axis. With this restriction Eqn. A-1 becomes:

$$T = \frac{1}{2}[M_F\,\dot{w}^2 + 2\,M_F e\,\dot{w}\dot{\theta} + (M_F e^2 + I_F)\dot{\theta}^2] + m\int_o^l [2\dot{w}^2 + \dot{h}^2$$

$$+ \dot{\theta}^2(z^2 + y^2\sin^2\Lambda + r_\alpha^2\cos^2\Lambda)]dy + m\int_o^l [2\,\dot{w}\dot{h} - 2\,\dot{w}\dot{\theta}(z + y\sin\Lambda)$$

$$- 2\dot{h}\dot{\theta}\,(z + y\sin\Lambda) + (2zy\sin\Lambda)\,\dot{\theta}^2]\,dy + M_S\,[\dot{w}^2 + 2\dot{h}\dot{w}$$

$$+ \dot{h}^2 - 2(z + l\sin\Lambda + x_s)\,\dot{\theta}\dot{w} - 2\,(z + l\sin\Lambda + x_s)\dot{h}\dot{\theta}$$

$$+ (z + l\sin\Lambda + x_s)^2\dot{\theta}^2 + I_S\,\dot{\theta}^2 \qquad \text{(A-3)}$$

In Eqn. A-3, use has been made of the fact that $\int_c \xi d\xi$ is to be zero for a uniformly distributed mass. In addition, the moment of inertia per unit length of the wing sections, about the y-axis, is $I_\alpha = mr_\alpha^2$ and the moment of inertia of the store is $I_s = M_s\,r_s^2$.

The mass matrix for the model is developed by first assuming a mode shape wing flexure, h(y, t). This shape function, f(y), is given as:

$$f(y) = \frac{1}{3}\,[6(y/l)^2 + 4(y/l)^3 + (y/l)^4] \qquad \text{(A-4)}$$

so that

$$h(y,t) = \bar{h}(t)f(y) \qquad \text{(A-5)}$$

the kinetic energy expression is now given as:

$$T = \frac{1}{2}\{(M_F + 2\,ml)\dot{w}^2\} + \frac{1}{2}\{I_F + M_F e^2\}$$

$$+ 2\,ml(z^2 + \frac{1}{3}\,l^2\sin^2\Lambda + r_\alpha^2\cos^2\Lambda + zl\sin\Lambda)\}\dot{\theta}^2$$

$$+ \frac{1}{2}\{2m\int_o^l f^2dy\}\,\dot{\bar{h}}^2 + \{2m\int_o^l f dy\}\dot{w}\dot{\bar{h}} \qquad \text{(A-6)}$$

$$+ \{M_F e - 2ml\,(z + \frac{1}{2}\,l\sin\Lambda)\}\dot{\theta}\dot{w} - \{2m\int_o^l (fz + fy\sin\Lambda)\,dy\}\dot{\theta}\dot{\bar{h}}$$

$$+ (z + l \sin\Lambda + x_s)^2\dot{\theta}^2] + M_s r_s^2 \dot{\theta}^2$$

Since the airplane motion is described by the coordinates w, θ, and $\bar{h}$, the mass matrix for the equations of motion for the model is developed by using the standard definition of M_{ij} in terms of partial derivatives of T.

$$M_{11} = \frac{\partial^2 T}{\partial \dot{w}^2} = M_F + 2ml + 2 M_S = M_T + 2M_S \tag{A-7}$$

$$M_{12} = \frac{\partial^2 T}{\partial \dot{w} \partial \dot{\bar{h}}} = 2m \int_o^l f dy + 2 M_S \tag{A-8}$$

$$M_{13} = \frac{\partial^2 T}{\partial \dot{w} \partial \dot{\theta}} = M_F e - 2\, ml(z + \frac{1}{2} l \sin\Lambda) \tag{A-9}$$

$$- 2M_S (z + l \sin\Lambda + x_s)$$

Because the reference system is centered at the aircraft center of mass, M_{13} is equal to zero. From statics the following equation for e is found:

$$e = 2 \frac{ml}{M_F} (z + \frac{1}{2} l \sin\Lambda) + 2 \frac{M_S}{M_F} (z + l \sin\Lambda + x_s) \tag{A-10}$$

The remaining mass matrix terms are:

$$M_{22} = \frac{\partial^2 T}{\partial \dot{\bar{h}}^2} = 2\, m \int_o^l f^2\, dy + 2\, M_S \tag{A-11}$$

$$M_{23} = \frac{\partial^2 T}{\partial \dot{\bar{h}} \partial \dot{\theta}} = - 2m \int_o^l f(z + y \sin\Lambda)\, dy \tag{A-12}$$

$$- 2\, M_S (z + l \sin\Lambda + x_s)$$

$$M_{33} = \frac{\partial^2 T}{\partial \dot{\theta}^2} = I_F + M_F e^2 + 2\, ml\, (z^2 + xl \sin\Lambda + \frac{1}{3} l^2 \sin^2\Lambda + r_o^2 \cos^2\Lambda)$$

$$+ 2\,M_S(z + l\,\sin\Lambda + x_s)^2 + 2\,M_S r_S^2 \qquad \text{(A-13)}$$

The elements on the mass matrix can be re-written by introducing non-dimensional parameters. These are:

$$\mu = \frac{2ml}{M_F} \qquad \text{(A-14)}$$

$$M_T = M_F\,(1 + \mu) \qquad \text{(A-15)}$$

$$\beta = \frac{M_S}{ml} \qquad \text{(A-16)}$$

These expressions are the result of non-dimensionalizing the equations of motion, as will be shown.

Strain Energy

The strain energy for the model consists of two parts, that due to the wing bending and that due to an artificial plunge spring, k. The plunge spring is present so that the effect on aircraft stability of restraining the plunge degree-of-freedom can be studied. The strain energy, U, is:

$$U = 2\,[\frac{1}{2}\int_o^l EI\,(f'')^2\,dy] + \frac{1}{2}\,kw^2 \qquad \text{(A-17)}$$

The wing cantilever natural frequency, ω_o, is introduced into the strain energy by noting that, for free vibration of the clamped wing only,

$$\frac{1}{2}\,(\bar{h})^2\int_o^l EI(f'')^2\,dy = \frac{1}{2}\,\bar{h}^2\,\omega_o^2\int_o^l mf^2 dy \qquad \text{(A-18)}$$

or

$$\frac{1}{2}(\bar{h})^2 \int_o^l EI\,(f'')^2\,dy = \frac{1}{2} m\omega_o^2 (\bar{h})^2 \int_o^l f^2\,dy \qquad \text{(A-19)}$$

thus,

$$U = 2\left[\frac{1}{2} m\omega_o^2 \int_o^l f^2\,dy\right]\bar{h}^2 + \frac{1}{2} kw^2 \qquad \text{(A-20)}$$

Generalized Forces

The aerodynamic forces acting upon the aircraft arise from the distributed airloads along the wings and the load from the canard surfaces. These loads are deformation dependent. Unsteady aerodynamic theory was used to develop expressions for the distributed wing lift and moment. These expressions according to Reference 4, are first written in terms of wing deflection, H, pitch, α, and derivatives $\sigma = dH/dy$, and $\tau = d\alpha/dy$. These expressions are:

$$L(y,t) = \pi\rho b^2 \{\ddot{H} + V\dot{\alpha}\cos\Lambda + V\sigma\sin\Lambda - ba\ddot{\alpha} - ba\,V\tau\sin\Lambda\} + 2\pi\rho b\,V\cos\Lambda\,C(k)\{\dot{H} + V\alpha\cos\Lambda + V\sigma\sin\Lambda + b\left(\frac{1}{2}-a\right)(\dot{\alpha} + V\tau\sin\Lambda)\} \qquad \text{(A-21)}$$

$$M_y(y,t) = -\pi\rho b^3 \{V\left(\frac{1}{2} - a\right)\dot{\alpha}\cos\Lambda + \frac{1}{2} V^2\tau\cos\Lambda\sin\Lambda - a\ddot{H} - Va\,\dot{\sigma}\sin\Lambda + b\left(\frac{1}{8} + a^2\right)(\ddot{\alpha} + V\dot{\tau}\sin\Lambda)\} + 2\pi\rho b^2 V\cos\Lambda\left(\frac{1}{2} + a\right)C(k)\{\dot{H} + V\alpha\cos\Lambda + V\sigma\sin\Lambda + b\left(\frac{1}{2} - a\right)(\dot{\alpha} + V\tau\sin\Lambda)\} \qquad \text{(A-22)}$$

The total wing deflection, H, and spanwise angle of attack are given by:

$$H = (x + y \sin\Lambda)\,\theta - h(y,t) - w \tag{A-23}$$

$$\alpha = \theta\cos\Lambda \tag{A-24}$$

The derivatives, with respect to y, are:

$$\sigma = \frac{\partial H}{\partial y} = \theta \sin\Lambda - \frac{dh}{dy} \tag{A-25}$$

$$\tau = \frac{\partial \alpha}{\partial y} = 0 \tag{A-26}$$

These expressions are substituted into Eqns. A-21 and A-22. The distributed lift and moment expressions become:

$$\begin{aligned} L(y,t) = \pi\rho b^2 \{&(x + y \sin\Lambda - ba \cos\Lambda)\,\ddot{\theta} - \ddot{h} - \dot{w} \\ &+ V\dot{\theta} - V \sin\Lambda \frac{d\dot{h}}{dy}\} + 2\,\pi\rho b\,(V^2\cos^2\Lambda)\,C(k) \\ &\{(x + y \sin\Lambda + b\,(\frac{1}{2} - a)\cos\Lambda)\,\dot{\theta}/(V\cos\Lambda) \\ &- \dot{h}/(V\cos\Lambda) - \dot{w}/(V\cos\Lambda) + \theta/\cos\Lambda - \tan\Lambda \frac{\partial h}{\partial y}\} \end{aligned} \tag{A-27}$$

$$\begin{aligned} M_y(y,t) = -\pi\rho b^3 \{&-Va\dot{\theta} + (V/2)\cos^2\Lambda\,\dot{\theta} + a\dot{w} + a\ddot{h} \\ &- (x + y \sin\Lambda)\,a\ddot{\theta} + Va \frac{\partial h}{\partial y} \sin\Lambda \\ &+ b\,(\frac{1}{8} + a^2)\,\ddot{\theta}\cos\Lambda\} \\ &+ 2\pi\rho b^2\,V^2\cos^2\Lambda\,C(k)\,\{\theta/\cos\Lambda - \frac{\partial h}{\partial y}\tan\Lambda\}\,(\frac{1}{2} + a) \end{aligned}$$

$$+ 2\pi\rho b^2 V \cos\Lambda \left(\frac{1}{2} + a\right) C(k) \{-\dot{h} - \dot{w} + (x + y \sin\Lambda)$$

$$+ b \left(\frac{1}{2} - a\right) \cos\Lambda)\dot{\theta}\} \qquad \text{(A-28)}$$

Virtual Work:

If the aircraft is given an arbitrary virtual displacement, consisting of δh, δw, $\delta\theta$, the virtual work done by the airloads on the wing is written as follows:

$$\delta W_e = [\int_o^l \{-L(x + y \sin\Lambda) + M \cos\Lambda\} dy]\delta\theta + [\int_o^l fL dy] \delta h$$

$$+ [\int_o^l L dy] \delta w \qquad \text{(A-29)}$$

The generalized forces to be used in the equations of motion are found from equation A-29. They are:

$$Q_\theta = \int_o^l [-L (x + y \sin\Lambda) + M \cos\Lambda] dy \qquad \text{(A-30)}$$

$$Q_h = \int_o^l fL dy \qquad \text{(A-31)}$$

$$Q_w = \int_o^l L dy \qquad \text{(A-32)}$$

Substituting the expressions for L, M, and f, and then performing the required integrations, the expressions for the generalized forces become:

$$Q_w = \pi\rho b^2 \{(xl + \frac{1}{2} l^2 \sin\Lambda - bal \cos\Lambda) \ddot{\theta} - \frac{2}{5} l \ddot{\bar{h}}$$

$$- l\ddot{w} + Vl\dot{\theta} - (V \sin\Lambda) \dot{\bar{h}}\}$$

$$Q_w = \pi\rho b^2 \{(xl + \frac{1}{2} l^2 \sin\Lambda - bal \cos\Lambda)\ddot{\theta} - \frac{2}{5} l \ddot{\bar{h}}$$

$$- l\ddot{w} + Vl\dot{\theta} - (V \sin\Lambda)\dot{\bar{h}}\}$$

$$+ 2\pi\rho bV \cos\Lambda\, C(k) \{(xl + \frac{1}{2} l^2 \sin\Lambda + bl(\frac{1}{2} - a)\cos\Lambda)\dot{\theta}$$

$$- \frac{2}{5} l\dot{\bar{h}} - l\dot{w} + lV\theta - (V \sin\Lambda)\bar{h}\} \qquad \text{(A-33)}$$

$$Q_h = \pi\rho b^2 l \{(\frac{2}{5}x + \frac{13}{45} l \sin\Lambda - \frac{2}{5} ba \cos\Lambda)\ddot{\theta}$$

$$- (\frac{104}{405})\ddot{\bar{h}} - \frac{2}{5}\ddot{w} + \frac{2}{5} V\dot{\theta} - \frac{1}{2} V \sin\Lambda \frac{\dot{\bar{h}}}{l}\}$$

$$+ 2\pi\rho bl (V \cos\Lambda)\, C(k) [(\frac{2}{5}x + \frac{13}{45} l \sin\Lambda$$

$$+ b(\frac{1}{2} - a)\frac{2}{5}\cos\Lambda)\dot{\theta} - \frac{104}{405}\dot{\bar{h}} - \frac{2}{5}\dot{w}$$

$$+ \frac{2}{5} V\theta - (\frac{1}{2l} V \sin\Lambda)\bar{h}] \qquad \text{(A-34)}$$

$$Q_\theta = -\pi\rho b^2 \{(x^2 l + xl^2 \sin\Lambda + \frac{1}{3} l^3 \sin^2\Lambda) - (ba \cos\Lambda)$$

$$(xl + \frac{1}{2} l^2 \sin\Lambda)]\ddot{\theta} - (\frac{2}{5}xl + \frac{13}{45} l^2 \sin\Lambda)\ddot{\bar{h}}$$

$$- (xl + \frac{1}{2} l^2 \sin\Lambda)\ddot{w} + (xl + \frac{1}{2} l^2 \sin\Lambda) V\dot{\theta}$$

$$- (Vx \sin\Lambda + \frac{3}{5} lV \sin^2\Lambda)\dot{\bar{h}}\}$$

$$- 2\pi\rho bV \cos\Lambda\, C(k) \{[(x^2 l + xl^2 \sin\Lambda + \frac{1}{3} l^3 \sin^2\Lambda)$$

$$- (Vx \sin\Lambda + \frac{3}{5} Vl \sin^2\Lambda)\, \bar{h}\}$$

$$- \pi\rho b^3 [(\frac{1}{2} Vl \cos^3\Lambda - Vla \cos\Lambda)\, \dot{\theta} + (al \cos\Lambda)\, \ddot{w}$$

$$+ (\frac{2}{5} al \cos\Lambda)\, \ddot{\bar{h}} - (xl \cos\Lambda + \frac{1}{2} l^2 \sin\Lambda \cos\Lambda)\, a\ddot{\theta}$$

$$+ (Va \sin\Lambda \cos\Lambda (\frac{3}{5}))\, \dot{\bar{h}} + (bl (\frac{1}{8} + a^2) \cos^2\Lambda)\, \ddot{\theta}]$$

$$+ 2\pi\rho b^2 V \cos\Lambda (\frac{1}{2} + a)\, C(k)\, \{-(\frac{2}{5} l \cos\Lambda)\, \dot{\bar{h}} \qquad \text{(A-35)}$$

$$- (l \cos\Lambda)\, \dot{w} + [(xl + \frac{1}{2} l^2 \sin\Lambda) \cos\Lambda + bl (\frac{1}{2} - a) \cos^2\Lambda]\, \dot{\theta}\}$$

The equations of motion for the airplane are now written as

$$[M_{ij}] \begin{Bmatrix} \ddot{w} \\ \ddot{\bar{h}} \\ \ddot{\theta} \end{Bmatrix} + [k_{ij}] \begin{Bmatrix} w \\ \bar{h} \\ \theta \end{Bmatrix} = \begin{Bmatrix} Q_w \\ Q_{\bar{h}} \\ Q_\theta \end{Bmatrix} \qquad \text{(A-36)}$$

Where $k_{ij} = 0$, except for the following two terms, found from the strain energy expression, U.

$$k_{11} = \frac{\partial^2 U}{\partial w^2} = k \qquad \text{(A-37)}$$

$$k_{22} = \frac{\partial^2 U}{\partial \bar{h}^2} = 2\, m\, \omega_o^2 \int_o^l f^2\, dy \qquad \text{(A-38)}$$

A set of non-dimensional coordinates, ξ, are defined by the following transformation.

$$\begin{Bmatrix} \xi_1 \\ \xi_2 \\ \xi_3 \end{Bmatrix} = \begin{bmatrix} 1/l & 0 & 0 \\ 0 & 1/l & 0 \\ 0 & 0 & 1 \end{bmatrix} \begin{Bmatrix} w \\ \bar{h} \\ \theta \end{Bmatrix} \tag{A-39}$$

Inverting this relationship we have:

$$\begin{Bmatrix} w \\ \bar{h} \\ \theta \end{Bmatrix} = \begin{bmatrix} l & 0 & 0 \\ 0 & l & 0 \\ 0 & 0 & 1 \end{bmatrix} \begin{Bmatrix} \xi_1 \\ \xi_2 \\ \xi_3 \end{Bmatrix} = [\psi] \{\xi\} \tag{A-40}$$

Equation A-36 is transformed as follows:

$$[\psi]^T [m] [\psi] \{\ddot{\xi}\} + [\psi]^T [k] [\psi] \{\xi\} = [\psi]^T \{Q\} \tag{A-41}$$

Each equation (row) is then divided by $M_T l^2$. Equation A-41 becomes:

$$[M_{ij}] \{\ddot{\xi}\} + [k_{ij}] \{\xi\} = (1/M_T l^2) [\psi]^T \{Q\} \tag{A-42}$$

At this point we use notation ($\bar{}$) above a variable to indicate division by l, e.g.

$$\bar{z} = z/l \qquad \bar{x}_s = x_s/l$$

Non-dimensional terms appearing in the equations of motion are: μ = wing mass/fuselage mass, β = store mass/wing mass. The non-dimensional elements of the mass matrix are:

$$M_{11} = 1 + \left(\frac{\mu\beta}{1+\mu}\right) \tag{A-43}$$

$$M_{12} = \frac{2}{5} \left(\frac{\mu}{1+\mu}\right) + \left(\frac{\mu\beta}{1+\mu}\right) \tag{A-44}$$

$$M_{13} = 0 \tag{A-45}$$

$$M_{13} = 0 \tag{A-45}$$

$$M_{22} = \frac{104}{405}\left(\frac{\mu}{1+\mu}\right) + \left(\frac{\mu\beta}{1+\mu}\right) \tag{A-46}$$

$$M_{23} = -\left(\frac{\mu}{1+\mu}\right)\left(\frac{2}{5}\,\bar{z} + \frac{13}{45}\sin\Lambda\right) \tag{A-47}$$

$$- \left(\frac{\mu\beta}{1+\mu}\right)\left(\bar{z} + \sin\Lambda + \bar{x}_s\right)$$

$$M_{33} = \frac{\bar{r}_o^2}{1+\mu} + \mu\left(\bar{z} + \frac{1}{2}\sin\Lambda\right)^2 + \left(\frac{\mu}{1+\mu}\right)\left(\frac{1}{12}\sin^2\Lambda + \right.$$

$$\left.\bar{r}_\alpha^2\cos^2\Lambda\right) + \left(\frac{\beta\mu}{1+\mu}\right)\bar{r}_s^2 + \left(\frac{2\mu^2\beta}{1+\mu}\right) \tag{A-48}$$

$$\left[\left(\bar{z} + \frac{1}{2}\sin\Lambda\right)^2 + \left(\bar{z} + \frac{1}{2}\sin\Lambda\right)\left(\bar{x}_s + \frac{1}{2}\sin\Lambda\right)\right]$$

$$+ \frac{\mu^2\beta^2}{1+\mu}\left(\bar{z} + \sin\Lambda + \bar{x}_s\right)^2$$

$$\bar{r}_o^2 = \frac{I_F}{M_F(1+\mu)l^2} \tag{A-49}$$

The non-zero terms of the non-dimensional stiffness matrix are:

$$k_{11} = k/M_T = \omega_p^2 \tag{A-50}$$

where ω_p is the uncoupled plunge natural frequency.

$$k_{22} = \omega_o^2\left[2(ml/M_T)\int_o^l f^2\,dy\right] = \omega_o^2\left(\frac{\mu}{1+\mu}\right)\left(\frac{104}{405}\right) \tag{A-51}$$

The generalized forces can be divided into two categories, the apparent mass,

following parameters, we can write these apparent mass and AIC terms in matrix form.

$$2\,b\ell = S \qquad D = \frac{\rho S C_{L_\alpha} V_n}{M_T}$$

$$a = -\frac{1}{2} \qquad \tilde{\mu} = \frac{\pi \rho S}{M_T} \bar{b}\ell$$

$$Q = \frac{2 q_n S C_{L_\alpha}}{M_T}\ell \qquad \bar{y} = (\bar{x} + \frac{1}{2}\sin\Lambda)$$

$$V\cos\Lambda = V_n$$

The elements of the apparent mass matrix are:

$$\tilde{M}_{11} = \tilde{\mu} \tag{A-52}$$

$$\tilde{M}_{12} = \frac{2}{5}\tilde{\mu} \tag{A-53}$$

$$\tilde{M}_{13} = -\tilde{\mu}\,(\bar{y} + \frac{1}{2}\bar{b}\cos\Lambda) \tag{A-54}$$

$$\tilde{M}_{22} = \frac{104}{405}\tilde{\mu} \tag{A-55}$$

$$\tilde{M}_{23} = -\tilde{\mu}(\bar{y} + \frac{2}{9}\sin\Lambda + \frac{1}{2}\bar{b}\cos\Lambda) \tag{A-56}$$

$$\tilde{M}_{33} = -\tilde{\mu}\,(\bar{y}^2 + \frac{1}{12}\sin^2\Lambda + \bar{y}\bar{b}\cos\Lambda + \frac{3}{8}\bar{b}^2\cos^2\Lambda) \tag{A-57}$$

$$\tilde{M}_{21} = \tilde{M}_{12} \tag{A-58}$$

$$\tilde{M}_{31} = \tilde{M}_{13} \tag{A-59}$$

$$\tilde{M}_{32} = \tilde{M}_{23} \tag{A-60}$$

The elements of the aerodynamic influence coefficient matrix are given as $\tilde{K}_{ij} + i\omega b_{ij}$. The elements of this matrix are listed below:

$$\tilde{K}_{11} = \tilde{K}_{21} = \tilde{K}_{31} = 0 \tag{A-61}$$

$$\tilde{K}_{12} = QC(k)/\tan\Lambda \tag{A-62}$$

$$\tilde{K}_{13} = -QC(k)/\cos\Lambda \tag{A-63}$$

$$\tilde{K}_{22} = \frac{1}{2} QC(k) \tan\Lambda \tag{A-64}$$

$$\tilde{K}_{23} = -\frac{2}{5} QC(k)/\cos\Lambda \tag{A-65}$$

$$\tilde{K}_{32} = -QC(k) \tan\Lambda \left(\bar{x} + \frac{3}{5} \sin\Lambda\right) \tag{A-66}$$

$$\tilde{K}_{33} = QC(k)\bar{y}/\cos\Lambda \tag{A-67}$$

$$b_{11} = DC(k) \tag{A-68}$$

$$b_{12} = D\left(\frac{1}{2}\bar{b} \tan\Lambda + \frac{2}{5} C(k)\right) \tag{A-69}$$

$$b_{13} = -D\left[\frac{1}{2} \bar{b} + C(k) (\bar{y} + \bar{b} \cos\Lambda)\right] \tag{A-70}$$

$$b_{21} = \frac{2}{5} DC(k) \tag{A-71}$$

$$b_{22} = D\left[\frac{1}{4} \bar{b} \tan\Lambda + \left(\frac{104}{405}\right) C(k)\right] \tag{A-72}$$

$$b_{23} = -D\left[\frac{1}{5} \frac{\bar{b}}{\cos\Lambda} + C(k) \frac{2}{5} \left(\bar{y} + \frac{2}{9} \sin\Lambda + \bar{b} \cos\Lambda\right)\right] \tag{A-73}$$

$$b_{31} = -DC(k)\, y \tag{A-74}$$

$$b_{32} = -D[\frac{1}{2}\, \bar{b}\, \tan\Lambda\, (y + \frac{1}{10}\, \sin\Lambda) + \tag{A-75}$$

$$\frac{2}{5}\, C(k)\, (y + \frac{2}{9}\, \sin\Lambda) + \frac{1}{4}\, \bar{b}^2\, \sin\Lambda]$$

$$b_{33} = D[\frac{\bar{b}}{2}\, (y/\cos\Lambda) + C(k)\, (y^2 + \frac{1}{12}\, \sin^2\Lambda + \bar{b}\, y\, \cos\Lambda)$$

$$-\frac{1}{2}\, \bar{b}^2\, \sin^2\Lambda] \tag{A-76}$$

APPENDIX B

Solution Methods

Two methods were used to solve the flutter problem. One method, called the P-K method, assumes a system response both at flutter and before and after flutter of the form e^{pt}, where p is a complex number. For simple harmonic motion at flutter the aerodynamic influence coefficients, which are derived from the generalized aerodynamic forces, are valid. With the P-K method, the eigenvalue equation is written as:

$$[p^2[M] + [K] - q_n[A]] \{\xi_i\} = \{0\} \tag{B-1}$$

The acrodynamic influence coefficients can be divided into real and imaginary parts. They are written as:

$$q_n[A] = q_n [Q_R] + p(\frac{q_n}{\omega}) [Q_I] \tag{B-2}$$

where [Q_R] and [Q_I] are the real and imaginary parts of [A], respectively. Substituting Eqn. (B-2) into Eqn. (B-1), we have:

$$[p^2[M] + [K] - q_n[Q_R] - p (\frac{q_n}{\omega}) [Q_I]] \{\xi_i\} = \{0\} \tag{B-3}$$

or

$$[p^2[M] + p[B]+[C]] \{\xi_i\} = \{0\} \tag{B-4}$$

where

$$[B] = -\left(\frac{q_n}{\omega}\right)[Q_I] = \frac{1}{2}\rho V_n \left(\frac{b}{k}\right)[Q_I] \tag{B-5}$$

and

$$[C] = [K] - q_n[Q_R] \tag{B-6}$$

The parameter k is called the reduced frequency and is given by:

$$k = \frac{\omega b}{V_n} \tag{B-7}$$

The method begins with the choice of an initial value of reduced frequency and a fixed value of velocity. This initial reduced frequency is a starting point for calculating the aerodynamic influence coefficients. A value of p is found from Eqn. (B-5). Recall that p is a complex number.

$$p = p_R + ip_I \tag{B-8}$$

From the imaginary part of p, a new value for reduced frequency can be calculated. This new value of reduced frequency generally will not match the initial guess for reduced frequency. Therefore, a "lining up" process of the input values k with the computed values of k is necessary. This lining up process continues until the input value of k matches the output value of k for a particular frequency. This process is then repeated for each modal frequency and for each velocity increment.

The other method used to solve the flutter problem is similar to the P-K method. Instead of using the unsteady Theodorsen aerodynamic formulation, as was used in the previous method, quasi-steady aerodynamics are used. In

quasi-steady aerodynamics, motion occurs very slowly such that reduced frequency can be taken as zero.

With this assumption, the eigenvalue equation is greatly simplified. Since reduced frequency is zero, the [Q_R] and [Q_I] matricies are independent of reduced frequency. The resulting eigenvalue equation is written as:

$$[p^2[M] + p[B] + [C]] \{\xi_i\} = \{0\} \tag{B-9}$$

where

$$[B] = -\frac{1}{2} \rho b V_n [\bar{Q}_I] \tag{B-10}$$

$$[C] = [K] - q_n[\bar{Q}_R] \tag{B-11}$$

The [$\bar{Q}_R$] and [$\bar{Q}_I$] matricies are the real and imaginary parts of [A] with the reduced frequency dependence removed.

Since Eqn. (B-10) is independent of reduced frequency, no frequency iteration is necessary, values for p can be calculated directly for a specific velocity.

or

END

FILMED

4-83

DTIC